Final Report for Period: 08/2010 - 07/2011
Submitted on: 09/14/2011
Principal Investigator: Dixon, David A.
Award ID: 0608896
Organization: U of Alabama Tuscaloosa
Submitted By:
Dixon, David - Principal Investigator
Title:
NIRT: Active Nanoparticles in Nanostructured Materials Enabling Advances in Renewable Energy and Environmental Remediation

Project Participants

Senior Personnel

Name: Dixon, David
Worked for more than 160 Hours: Yes
Contribution to Project:

Name: Gole, James
Worked for more than 160 Hours: Yes
Contribution to Project:

Name: Szulczewski, Gregory
Worked for more than 160 Hours: Yes
Contribution to Project:

Name: Fedorov, Andrei
Worked for more than 160 Hours: Yes
Contribution to Project:

Name: Burda, Clemens
Worked for more than 160 Hours: Yes
Contribution to Project:

Post-doc

Graduate Student

Name: Wang, Tsang-Hsiu
Worked for more than 160 Hours: Yes
Contribution to Project:
graduate student doing computational chemistry calculations on nanoclusters

Name: Corno, James
Worked for more than 160 Hours: Yes
Contribution to Project:
grad student Georgia Tech Physics

Name: Ozdemir, Serdar
Worked for more than 160 Hours: Yes
Contribution to Project:
grad student Georgia Tech Physics

Name: Ogden, Andrew
Worked for more than 160 Hours: Yes

Contribution to Project:
grad student Georgia Tech Engineering

Name: Brauer, Jon
Worked for more than 160 Hours: Yes
Contribution to Project:
graduate student at UA working on experimental effort.

Name: Fang, Zongtang
Worked for more than 160 Hours: Yes
Contribution to Project:

Undergraduate Student

Name: Ball, Caroline
Worked for more than 160 Hours: Yes
Contribution to Project:
Computer Based Honors Project student doing computational chemistry calculations on nanoclusters - no formal support as this is part of a class

Name: Campbell, Jenna
Worked for more than 160 Hours: Yes
Contribution to Project:
undergraduate student Georgia Tech Physics

Name: Laminack, William
Worked for more than 160 Hours: Yes
Contribution to Project:
undergraduate student Georgia Tech Physics

Name: Papadimitriou, Charalampos (Ha
Worked for more than 160 Hours: Yes
Contribution to Project:
undergraduate student Georgia Tech Physics

Name: De Niro, Matthew
Worked for more than 160 Hours: Yes
Contribution to Project:
undergrad at Ga Tech in physics working on experimental aspects of the project.

Name: Hennigan, Jamie
Worked for more than 160 Hours: Yes
Contribution to Project:

Name: Waymans, Emily
Worked for more than 160 Hours: No
Contribution to Project:

Name: Gist, Natalie
Worked for more than 160 Hours: Yes
Contribution to Project:
Undergraduate research through Computer Based Honors Program (CBHP) at UA.

Name: Guenther, Courtney
Worked for more than 160 Hours: Yes

Contribution to Project:

Name: Smith, Kyle
Worked for more than 160 Hours: Yes
Contribution to Project:

Technician, Programmer

Other Participant

Research Experience for Undergraduates

Organizational Partners

Georgia Institute of Technology

Case Western Reserve University

Other Collaborators or Contacts

Naval Research Laboratory - Discuss Research on metal oxides, catalysis, and sensors

Activities and Findings

Research and Education Activities: (See PDF version submitted by PI at the end of the report)

Findings: (See PDF version submitted by PI at the end of the report)

Training and Development:
Undergraduate and graduate students are part of an interdisciplinary team focused on the study of active nanoparticles using experimental and computational approaches. The research personnel who are participating in this project are benefiting from the interaction of researchers in different disciplines including physics, chemistry, and engineering and at different university sites. They are being educated in the design and completion of experiments and computations to understand the active nature of these nanoparticles. They are learning about catalysis and reactor design and are being exposed to a wide variety of materials synthesis and characterization techniques. Since the project requires essential elements of chemical and mechanical engineering, physics, and chemistry, namely reactor design, microfabrication, surface and spectroscopic analysis, and coordinated testing, the overall effort offers significant opportunities for basic science discovery coupled to real world applications.

As an example, undergraduate and graduate students have learned about computational chemistry, especially electronic structure theory and density functional theory, and high performance computing. They have also learned about graphical user interfaces and how to design posters to present their material. They have also been involved in writing papers.

There are 8 graduate students (3 women, 1 minority) in the Dixon research group. There are two postdoctoral fellows (1 woman) in the group during the previous year.

There is a significant undergraduate research component to the project at Georgia Tech and at The University of Alabama (UA). At UA, a number of undergraduate students from the Computer Based Honors Program (CBHP) are involved in the research effort. They are performing high level electronic structure calculations on advanced computer architectures so that we can understand how to make reliable predictions of the energetics of nanostructures. The students have been involved in University and System wide poster presentations as well as in presentations to their CBHP peers. The Gole group has 6 undergraduates, 2 of whom are women. The Dixon group sponsored 6 REU students

(2 women) from non REU funding during the summer of 2010. The Dixon group had 9 undergraduate students (1 woman) in the Fall 2010 and Spring 2011 semesters. Two undergraduates (1 woman) won two of the 3 upper level UA Chemistry Department Awards. Two students (1 woman) were named Goldwater Scholars. Five of the 15 Randall Undergraduate Research Awards were awarded to students working in the Dixon group including 3 women and one student was awarded the Pettus Randall Scholarship for outstanding research by a student in the Computer Based Honors Program at UA.

Ideas about nanoscience and ethical issues in science and engineering were presented to REU students at UA during the Summer of 2010. We are running a Freshman Learning Community at UA in the Fall of 2011 with a focus on energy and the environment. We are expanding our discussions of the role of nanoscience in modern society and the need for scientists and engineers with multidisciplinary skill sets. We are designing a freshman chemistry laboratory using nanoparticles demonstrate the particle-in-a-box. We are improving the computational chemistry laboratories in the Honors Freshman Chemistry and junior Physical Chemistry courses. In the Fall, 2010, about 120 Freshman Chemistry Honors students did a laboratory in computational chemistry in the Dixon group studying H2 storage and release at the molecuar/nano scale.

Outreach Activities:

Presentations 2010 - 2011:

Ogden, A., Gole, J. L., Fedorov, A. G., 'Hybrid Nanostructured TiO2 Electrodes for Photocatalytic Hydrogen Production', 3rd Annual GCOE International Energy Conference, Ishigaki, Japan, Dec. 9-14, 2010.

Gole, J. L.; Ozdemir, S., ' Novel Concept for the Formation of Sensitive, Selective, Rapidly Responding Conductometric Sensors', Microfabricated and Nanofabricated Systems for MEMS/NEMS 9, 218th Electrochemical Society Meeting, Oct. 10-15, 2010, Las Vegas, NV.

Gole, J. L.; Ozdemir, S., 'Nanostructure Directed Gas-Surface Physisorption Based on Selective Modification of Nanopore Coated Micropores', Pits and Pores, New Materials and Applications 218th Electrochemical Society Meeting, Oct. 10-15,2010, Las Vegas, NV.

Gole, J. L., 'Selectivity Improvements and Response Time Scale of Porous Silicon Conductometric Gas Sensors', 218th Electrochemical Society Meeting, Oct. 10-15,2010, Las Vegas, Neveda, in Chemical Sensors 9- Chemical and Biological Sensors and Analytical Systems

Gole, J. L., 'Active Nanostructure Directed Processes at Interfaces': Speaker and Session Chair, Nanopackaging, ' A General Model for Sensor and Microreactor Design on Semiconductor Interfaces', Nanoporous Materials, Nano Science and Technology- Dalian, China, October 23-26,2011, Keynote.

Gole, J. L., 'Active Nanostructure Directed Processes at Interfaces'Villa Conference on Interactions Among Nanostructures, April 21-25, 2011,Las Vegas, Nevada, Invited Talk,

Dixon, D. A. 'Computational Chemistry Undergraduate Research at UA,' High School Advisory Board, The University of Aalabama, Sept. 13, 2010.

Dixon, D. A., 'Computational Chemistry in a Distributed Computing Environment,' University of Alabama-Birmingham, Cyberinfrastructure Day, 2010, Birmingham, AL, September, 15, 2010, Invited Lecture.

Dixon, D. A., Chen, M.; Stott, A.C.; Li, S. 'Management of Computational Chemistry Electronic Structure Data in the U.S.', ZCAM Workshop on Databases in quantum chemistry: Validation of methods and software and repositories of reference computational results, Zaragoza Spain, Sept. 22-24, 2010, Invited Lecture

Dixon, D. A. 'Reliable prediction of molecular properties of fluorinated inorganic compounds', Symposium on Fundamental and Applied Inorganic Fluorine Chemistry and Their Impacts on Energy Conservation and the Environment, PacifiChem 2010, Honolulu, HI, Dec. 15-20, 2010. Invited Lecture.

Christe, K. O.; Dixon, D. A.; Grant, D. J.; Tham, F. S.; Vij, A.; Vij, V.; Wang, T.-H.; Wilson, W. W. "Dinitrogen Difluoride Chemistry. Improved Syntheses of cis? and trans?N2F2 , Synthesis and Characterization of N2F+Sn2F9-, Ordered Crystal Structure of N2F+Sb2F11-, High-Level Electronic Structure Calculations of cis-N2F2, trans-N2F2, F2N=N, and N2F+, and Mechanism of the trans-cis Isomerization of N2F2 Symposium on Fundamental and Applied Inorganic Fluorine Chemistry and Their Impacts on Energy Conservation and the Environment, PacifiChem 2010, Honolulu, HI, Dec. 15-20, 2010. Invited Lecture.

Dixon, D. A.; Christe, K. O.; Vasiliu, M.; Craciun, R.; Li, S.; Grant, D. J.; Jackson, V. E., 'Recent Results on the Lewis Acidity Scale: Quantitative Fluoride Affinities', 20th Winter Fluorine Conference, St. Petersburg Beach, FL, Jan. 9-14, 2011. Invited Lecture.

Haiges, R.; Christe, K. O.;, Boatz, J. A.; Dixon, D. A., 'Metal Fluorides as Precursors for Environmental Friendly Energetic Materials: Replacements for Lead Diazide,' 20th Winter Fluorine Conference, St. Petersburg Beach, FL, Jan. 9-14, 2011. Invited Lecture.

Christe, K. O.; Dixon, D. A.; Grant, D. J.; Wang, T.-H.; Vasiliu, M., 'Formation mechanism of NF4 + salts,' 20th Winter Fluorine Conference, St. Petersburg Beach, FL, Jan. 9-14, 2011. Invited Lecture

Vasiliu, M.; Arduengo, A. J. III; Dixon, D. A., 'Bond Energies in Models of the Schrock and Grubbs Metathesis Catalysts', 20th Winter Fluorine Conference, St. Petersburg Beach, FL, Jan. 9-14, 2011. Poster

Jackson, V. E.; Dixon, D. A.; Christe, K. O., 'Thermochemical Properties of Seleniumoxofluorides', 20th Winter Fluorine Conference, St. Petersburg Beach, FL, Jan. 9-14, 2011. Poster

Dixon, D. A.; 'Computational Studies of Catalytic Processes on Metal Oxides', Gordon Research Conference: Chemical Reactions at Surfaces, Feb. 6-11, 2011, Ventura CA, Invited Lecture

Dixon, D. A., 'Reliable predictions of the properties of transition metal complexes and fluorinated compounds,' Computers in Chemistry Division: ACS Award for Computers in Chemical and Pharmaceutical Research Award: Symposium in Honor of Thom Dunning, 241st ACS National Meeting, Anaheim, CA, Mar. 27-31, 2011. Invited Lecture

Dixon, D. A., 2011 SETCA Annual Meeting, Mississippi State, Starksville MS May 13-14, 2011. Invited Lecture

Dixon, D. A., LANSCE Summer School, Los Alamos National Lab, Los Alamos, NM, July 12-22, 2011, Invited Lecture.

Stott, A. C.; Abel, P. B.; DellaCorte, C.; Pepper, S. V.; Dixon, D. A., 'Computational Studies of the NiTi Alloy System: Bulk, Supercell, and Surface Calculations', Fall 2010 MRS Meeting, Boston MA.

Li, S.; Kelley, M. S.; Guenther, C. L.; Dixon D. A., 'Hydrolysis of Group VIB Transition Metal Oxide Clusters and Their Catalytic Activity in Methanol Partial Oxidation by Molecular Oxygen,' Joint SERM/SWRM 2010 Regional ACS meeting, New Orleans, LA, Nov. 30-Dec. 4, 2010.

Wang, T.-H.; Fang, Z.; Gist, N. W.; Li, S.; Dixon, D. A.,' Computational Study of the Hydrolysis Reactions of the Ground and First Excited Triplet States of Small TiO2 Nanoclusters', Joint SERM/SWRM 2010 Regional ACS meeting, New Orleans, LA, Nov. 30-Dec. 4, 2010, Poster

Journal Publications

Gole, JL; Prokes, SM; White, MG; Wang, TH; Craciun, R; Dixon, DA, "Evidence for high spin transition metal ion induced infrared spectral enhancement", JOURNAL OF PHYSICAL CHEMISTRY C, p. 16871, vol. 111, (2007). Published, 10.1021/jp075712

A. Ogden, J.L. Gole, and A.G. Fedorov, "Optical and Electronic Properties of Semiconducting Nanostructures for Photocatalytic Hydrogen Generation", J. Nanoelectronics and Optoelectronics I, p. 269, vol. 2, (2007). Published,

Jenna Campbell, James A. Corno, Nicole Larsen, and James L. Gole, "Development of Porous Silicon-based Active Microfilters", J. Electrochem. Soc, p. D128, vol. 155, (2008). Published,

James L. Gole, Sharka M. Prokes, and Orest J. Glembocki, "Efficient Room Temperature Conversion of Anatase to Rutile TiO2 Induced by High Spin Ion Doping", J. Phys. Chem. C, p. 1782, vol. 112, (2008). Published,

James A. Corno, John Stout, Rusen Wang, and James L. Gole, "Diffusion Controlled Self-Assembly and Dendritic Formation in Silver Seeded Anatase Titania Nanospheres", J. Phys. Chem. C, p. 5439, vol. 112, (2008). Published,

D. J. Grant, M. H. Matus, J. Switzer, D. A. Dixon, J. S. Francisco, and K.O. Christe, "Bond Dissociation Energies in Second Row Compounds", J. Phys Chem A, p. 3145, vol. 112, (2008). Published,

H. Wan, S. Li, T. A. Konovalova, S. Shuler, D. A. Dixon, and S. C. Street, "Experimental and Theoretical Studies of the Photoreduction of Copper(II)-Dendrimer Complexes", J. Phys. Chem C, p. 1335, vol. 112, (2008). Published,

A. Ogden, A. Fedorov, J.-i. Hong, and J. L. Gole, "Maintaining Particle Size in the Transformation of Anatase to Rutile Titania Nanospheres", J. Phys & Chem. of Solids, p. 2898, vol. 69, (2008). Published,

S. Ozdemir and J. L. Gole, "The Potential of Porous Silicon Gas Sensors", Current Opinions in Solid State and Materials Science, p. 92, vol. 11, (2008). Published,

J. L. Gole, S.M. Prokes, and M. G. White, "Metal Ion Induced Room Temperature Phase Transformation and Stimulated Infrared Spectroscopy on TiO2-based Surfaces", Appl. Surf. Sci., p. 718, vol. 255, (2008). Published,

S. Ozdemir and J.L. Gole, "Porous Silicon Gas Sensors for Room Temperature Detection of Ammonia and Phosphine", Chemical Sensors 8: Chemical (Gas, Ion, Bio) Sensors and Analytical Systems, ECS Transactions, p. 379, vol. 16, (2008). Published,

R. Giuly, J. A. Corno, and J. L. Gole, "A Simple Method of Generating Nano-pillars and Uniformly Separated Nano-needle Arrays on Silicon", Materials Lett., p. 2704, vol. 62, (2008). Published,

J. Baxter, Z. Bian, G. Chen, D. Danielson, M. Dresselhaus, A.G. Fedorov, T. Fisher, C. Jones, E. Maginn, U. Kortshagen, A. Manthiram, A Nozik, D. Rolison, T. Sands, L. Shi, L., D. Sholl, and Y. Wu, "Nanoscale design to enable the revolution in renewable energy", Energy & Environmental Science, p. , vol. , (2009). Accepted, 10.1039/B821698C

C. Mao, Y. Zhao, Yixin; X. Qiu, J. Zhu, and C. Burda, "Synthesis, characterization and computational study of nitrogen-doped CeO2 nanoparticles with visible-light activity", Phys. Chem. Chem. Phys., p. 5633, vol. 10, (2008). Published,

Y. Zhao, H. Pan, Y. Lou, X. Qiu, J. Zhu, and C. Burda, "Plasmonic Cu2-xS Nanocrystals: Optical and Structural Properties of Copper-Deficient Copper(I) Sulfides", J. Am. Chem. Soc., p. 4253, vol. 131, (2009). Published,

Y. Zhao, P. Larimer, R. T. Pressler, B. W. Strowbridge, and C. Burda, "Wireless Activation of Neurons in Brain Slices Using Nanostructured Semiconductor Photoelectrodes", Angew.Chem. Int. Ed., p. 2407, vol. 48, (2009). Published,

S. Li and D. A. Dixon, "Molecular Structures and Energetic of the (TiO2)n (n = 1???4) Clusters and Their Anions", J. Phys. Chem. A, p. 6646, vol. 112, (2008). Published,

M.H. Matus, M. T. Nguyen, K. A. Peterson, J. S. Francisco, and D. A. Dixon, "ClClO2 Is the Most Stable Isomer of Cl2O2. Accurate Coupled Cluster Energetics and Electronic Spectra of Cl2O2 Isomers", J. Phys. Chem. A, p. 9623, vol. 112, (2008). Published,

H. Wan, S. Li, T. A. Konovalova, Y. Zhou, J. S. Thrasher, D. A. Dixon, and S. C. Street, "Experimental and Theoretical Studies of the Photoreduction of Metal Ion-Dendrimer Complexes: Observation of a Delocalized Organic Radical", J. Phys. Chem. C, p. 5358, vol. 113, (2009). Published,

D. Tapu, D. A. Dixon, and C. Roe, "13C Spectroscopy of ???Arduengo-type??? Carbenes and Their Derivatives", Chem. Rev, p. , vol. , (2009). Accepted, 10.1021/cr800521g

J. L. Gole, J. Corno, S. Ozdemir, S. Prokes, and H.-C. Shin, "Active Microfiltered Sensor Interfaces, Phontocatalytic Reactors, and Microbattering Using Combined Micro/nanoporous Interfaces", Phys. Stat. Solid, p. , vol. , (2009). Accepted,

T. A. Konovalova, S. Li, N. E. Polyakov, A. L. Focsan, D. A. Dixon, and L. D. Kispert, "Measuring Ti(III)???Carotenoid Radical Interspin Distances in TiMCM-41 by Pulsed EPR Relaxation Enhancement Method", J. Phys. Chem. B, p. , vol. , (2009). Accepted,

James L. Gole, James Corno, Serdar Ozdemir, Sharka Prokes, and Heon-Cheol Shin, "Active Microfiltered Sensor Interfaces, Photocatalytic Reactors, and Microbatteries Using Combined Micro/nanoporous Interfaces", Phys. Stat. Solid, p. 1773, vol. 6, (2009). Published,

Daniel J. Grant, David A. Dixon, Joseph S. Francisco, David Feller, and Kirk A. Peterson, "Heats of Formation of the H1,2OmSn (m, n = 0 ??? 3) Systems from Electronic Structure Calculations", J. Phys. Chem. A, p. 11343, vol. 113, (2009). Published,

Tatyana A. Konovalova, Shenggang Li, Nikolay E. Polyakov, A. Ligia Focsan, David A. Dixon, and Lowell D. Kispert, "Measuring Ti(III)???Carotenoid Radical Interspin Distances in TiMCM-41 by Pulsed EPR Relaxation Enhancement Method", J. Phys. Chem. B, p. 8704, vol. 113, (2009). Published,

Amanda C. Stott, Phillip B. Abel, Guillermo H. Bozzolo, and David A. Dixon, "Interfacial Phase Stability in TiV Multi-Laminate Thin Films", J. Phys. Chem. C, p. 21383, vol. 113, (2009). Published,

Daniela Tapu, David A. Dixon, and Christopher Roe, "13C Spectroscopy of ???Arduengo-type??? Carbenes and Their Derivatives", , Chem. Rev, p. 3385, vol. 109, (2009). Published,

Changjie Mao, Yixin Zhao, Xiaofeng Qiu, Junjie Zhu, Clemens Burda, "Synthesis and characterization of nitrogen-doped SnO2 and comparison to nitrogen-doped CeO2 nanoparticles for visible-light applications", ECS Transactions, p. 67, vol. 16(15), (2009). Published,

Daniel J. Grant, Edward B. Garner III, Myrna H. Matus, Minh T. Nguyen, Kirk A. Peterson, Joseph S. Francisco, and David A. Dixon, "Thermodynamic Properties of the XO2, X2O, XYO, X2O2, and XYO2 (X, Y = Cl, Br and I) Isomers", J. Phys. Chem. A, p. 4254, vol. 114, (2010). Published,

Monica Vasiliu, Shenggang Li, Kirk A. Peterson, James L. Gole, and David A. Dixon, "Structure and Heats of Formation of Simple Alkali Metal Compounds: Hydrides, Chlorides, Fluorides, Hydroxides, and Oxides for Li, Na. and K", J. Phys. Chem. A, p. 4272, vol. 114, (2010). Published,

Guo-Xi Liang, Ling-Ling Li, Hong-Yin Liu, Jian-Rong Zhang, Clemens Burda, Jun-Jie Zhu, "Fabrication of near-infrared-emitting CdSeTe/ZnS core/shell quantum dots and their electrogenerated chemiluminescence", Chem. Comm, p. 2974, vol. 46, (2010). Published,

James L. Gole, Sharka M. Prokes, Xiaofeng Qiu, Clemens Burda, and Orest J. Glembocki, "Study of Concentration-dependent Cobalt Ion Doping of TiO2 and TiO2-xNx at the Nanoscale", Nanoscale, p. , vol. , (2010). Published, 10.1039/c0nr00125b

Yixin Zhao, Jeffrey S. Dyck, Brett M. Hernandez, and Clemens Burda, "Enhancing thermoelectric performance of ternary nanocrystals through adjusting carrier concentration", J. Am. Chem. Soc, p. 4982, vol. 132, (2010). Published,

Xiaofeng Qiu, Yixin Zhao, Ian M. Steward; Jeffrey S. Dyck, Clemens Burda, "Improvement of the thermoelectric power factor through anisotropic growth of nanostructured PbSe thin films", Dalton Trans, p. 1095, vol. 39, (2010). Published,

Yu Cheng, Anna C. Samia, Jun Li, Malcolm E. Kenney, Andrew Resnick, and Clemens Burda, "Delivery and Efficacy of a Cancer Drug as a Function of the Bond to the Gold Nanoparticle Surface", Langmuir, p. 2248, vol. 26, (2010). Published,

James L. Gole and Serdar Ozdemir, "Nanostructure Directed Physisorption vs Chemisorption at Semiconductor Interfaces: The Inverse of the Hard-Soft Acid-Base (HSAB) Concept", Chem Phys Chem, p. , vol. , (2010). Accepted,

Wang, TH; Navarrete-Lopez, AM; Li, SG; Dixon, DA; Gole, JL, "Hydrolysis of TiCl4: Initial Steps in the Production of TiO2", JOURNAL OF PHYSICAL CHEMISTRY A, p. 7561, vol. 114, (2010). Published, 10.1021/jp102020

Stott, AC; Brauer, JI; Garg, A; Pepper, SV; Abel, PB; DellaCorte, C; Noebe, RD; Glennon, G; Bylaska, E; Dixon, DA, "Bonding and Microstructural Stability in Ni55Ti45 Studied by Experimental and Theoretical Methods", JOURNAL OF PHYSICAL CHEMISTRY C, p. 19704, vol. 114, (2010). Published, 10.1021/jp103552

Li, KJ; Li, SG; Li, N; Dixon, DA; Klein, TM, "Tetrakis(dimethylamido)hafnium Adsorption and Reaction on Hydrogen Terminated Si(100) Surfaces", JOURNAL OF PHYSICAL CHEMISTRY C, p. 14061, vol. 114, (2010). Published, 10.1021/jp101363

Wang, TH; Dixon, DA; Henderson, MA, "C-C and C-Heteroatom Bond Dissociation Energies in CH3R ' C(OH)(2): Energetics for

Photocatalytic Processes of Organic Diolates on TiO2 Surfaces", JOURNAL OF PHYSICAL CHEMISTRY C, p. 14083, vol. 114, (2010). Published, 10.1021/jp102469

Wang, TH; Fang, ZT; Gist, NW; Li, SG; Dixon, DA; Gole, JL, "Computational Study of the Hydrolysis Reactions of the Ground and First Excited Triplet States of Small TiO2 Nanoclusters", JOURNAL OF PHYSICAL CHEMISTRY C, p. 9344, vol. 115, (2011). Published, 10.1021/jp111026

Gole, JL; Ozdemir, S, "Nanostructure-Directed Physisorption vs Chemisorption at Semiconductor Interfaces: The Inverse of the HSAB Concept", CHEMPHYSCHEM, p. 2573, vol. 11, (2010). Published, 10.1002/cphc.20100024

Vasiliu, M; Feller, D; Gole, JL; Dixon, DA, "Structures and Heats of Formation of Simple Alkaline Earth Metal Compounds: Fluorides, Chlorides, Oxides, and Hydroxides for Be, Mg, and Ca", JOURNAL OF PHYSICAL CHEMISTRY A, p. 9349, vol. 114, (2010). Published, 10.1021/jp105065

Christe, KO; Dixon, DA; Grant, DJ; Haiges, R; Tham, FS; Vij, A; Vij, V; Wang, TH; Wilson, WW, "Dinitrogen Difluoride Chemistry. Improved Syntheses of cis- and trans-N2F2, Synthesis and Characterization of N2F+Sn2F9-, Ordered Crystal Structure of N2F+Sb2F11-, High-Level Electronic Structure Calculations of cis-N2F2, trans-N2F2, F2N = N, and N2F+, an", INORGANIC CHEMISTRY, p. 6823, vol. 49, (2010). Published, 10.1021/ic100471

Christe, KO; Haiges, R; Boatz, JA; Jenkins, HDB; Garner, EB; Dixon, DA, "Why Are [P(C6H5)(4)]N-+(3)- and [As(C6H5)(4)]N-+(3)- Ionic Salts and Sb(C6H5)(4)N-3 and Bi(C6H5)(4)N-3 Covalent Solids? A Theoretical Study Provides an Unexpected Answer", INORGANIC CHEMISTRY, p. 3752, vol. 50, (2011). Published, 10.1021/ic200107

Wang, TH; Gole, JL; White, MG; Watkins, C; Street, SC; Fang, ZT; Dixon, DA, "The surprising oxidation state of fumed silica and the nature of water binding to silicon oxides and hydroxides", CHEMICAL PHYSICS LETTERS, p. 159, vol. 501, (2011). Published, 10.1016/j.cplett.2010.11.01

Grant, DJ; Wang, TH; Vasiliu, M; Dixon, DA, "F+ and F- Affinities of Simple NxFy and OxFy Compounds", INORGANIC CHEMISTRY, p. 1914, vol. 50, (2011). Published, 10.1021/ic102310

Ozdemir, S; Gole, JL, "A phosphine detection matrix using nanostructure modified porous silicon gas sensors", SENSORS AND ACTUATORS B-CHEMICAL, p. 274, vol. 151, (2010). Published, 10.1016/j.snb.2010.08.01

Wang, JW; Mao, BD; Gole, JL; Burda, C, "Visible-light-driven reversible and switchable hydrophobic to hydrophilic nitrogen-doped titania surfaces: correlation with photocatalysis", NANOSCALE, p. 2257, vol. 2, (2010). Published, 10.1039/c0nr00313

Ozdemir, S; Osburn, TB; Gole, JL, "Nanostructure Modified Gas Sensor Detection Matrix for NO Transient Conversion of NO to NO2", JOURNAL OF THE ELECTROCHEMICAL SOCIETY, p. J201, vol. 158, (2011). Published, 10.1149/1.358336

Christe, KO; Dixon, DA; Haiges, R; Hopfinger, M; Jackson, VE; Klapotke, TM; Krumm, B; Scherr, M, "Selenium(IV) fluoride and oxofluoride anions", JOURNAL OF FLUORINE CHEMISTRY, p. 791, vol. 131, (2010). Published, 10.1016/j.jfluchem.2010.04.00

Books or Other One-time Publications

D.A. Dixon, "Noble Gas Compounds: Reliable Computational Methods", (2009). Book, Published
Editor(s): E.I. Solomon, R.B. King, and R.A. Scott
Collection: Comprehensive Inorganic and Bioinorganic Chemistry
Bibliography: John Wiley & Sons

P. A. Kottle, A. G. Fedorov, and J. L. Gole, "Multiscale Mass Transport in Porous Silicon Gas Sensors", (2009). Book, Published
Editor(s): M. Schlesinger
Collection: Modern Aspects of Electrochemistry, Volume 43

Bibliography: pp 139-168
Springer

Gole, J. L.; Ozdemir, S., "Efficient Nanostructure Modified Interfaces for Array-based Sensing Based on the Novel Application of Hard/Soft Acid/Base Interactions", (2011). journal, Published
Collection: Physica Status Solidi C
Bibliography: volume 8, pp 1833-1836

Gole, J. L; Ozdemir, S., "Novel Concept for the Formation of Sensitive, Selective, Rapidly Responding Conductometric Sensors", (2010). journal, Published
Collection: MRS Proceedings
Bibliography: 1253-K07-05

Gole, J. L.; Ozdemir, S.; Prokes, S. M.; Dixon, D. A., "Active Nanostructures at Interfaces for Photocatalytic Reactors and Low-power Consumption Sensors", (2010). journal, Published
Collection: MRS Proceedings
Bibliography: 1257-O09-04

Li, K.; Li, S.; Li, N.; Klein, T. M. Dixon, D. A., "Tetrakis(ethylmethylamido) Hafnium Adsorption and Reaction on Hydrogen-Terminated Si(100) Surfaces", (2011). journal, awaiting print publication. on WEB
Collection: Journal of Physical Chemistry C
Bibliography: WEB ASAP 8 2011 DOI: 10.1021/jp111600v

Li, K.; Zhang, L.; Dixon, D. A.; Klein, T. M., "Undulating Topography for HfO2 Thin Films Deposited in a Meso-Scale Reactor using Hafnium (IV) tert butoxide", (2011). journal, awaiting print version, published on the WEB
Collection: AIChE Journal
Bibliography: WEB Online Feb. 16, 2011 DOI: 10.1002/aic.12504

Web/Internet Site

Other Specific Products

Contributions

Contributions within Discipline:

We are developing new approaches to the synthesis of nanoparticles. We are continuing to generate new developments in the synthesis of novel doped TiO2 nanoparticles, which promise to have novel properties. We have generalized the method for nitrogen doping of TiO2 to other metal oxides including Faujasite, silica, and alumina as well as CeO2. We have expanded the idea of doped nanomaterials to chalcogenides. This extends this important technique to other materials. This has enabled us to develop a broader understanding of the electronic effects of doping of metal oxides.

We have demonstrated visible-light-driven reversible and switchable hydrophobic to hydrophilic nitrogen doped titania surfaces and showed that this behavior correlates with photocatalysis. This offer a new way to consider probing surfaces for catalytic activity and show the role of water on the surface.

We have developed an entirely new approach to the design of novel, highly sensitive sensors and catalysts based on the inverse hard/soft acid base model (IHSAB). When coupled with the intrinsic properties of semiconductors, this model provides a fundamental new way to design sensors based on their ability to adsorb/desorb species and the way that electron injection can change the resistance of the material.

We have developed an improved understanding of an impact of the spray cooling of the electrode support surface upon deposition of nanoparticles during the formation of the Hybrid NanoPatterned and Spray-Coated Electrode (HNPSCE) structure. The new new HNPSCE electrode structure demonstrated enhanced photocatalytic operational stability and hydrogen generation yield with new HNPSCE electrode

structure. We have developed new understanding of the mechanical and electrical properties of the HNPSCE system on the nanoscale, as related to electrode structural morphology and processing parameters.

Nitrogen-doped TiO2 nanoparticles have been synthesized using sol-gel methods and subsequently transformed into anatase nanocubes at room temperature by aging in acidic solutions of NaF. This two-step synthesis allows for independent control over the dopant concentration and material morphology. The approach is simple and could advance the preparation of visible light active TiO2 photocatalysts.

We have predicted complete sets of reliable thermodynamic properties of alkaline metal compounds for modeling furnaces and high temperature combustion systems.

We have continued to develop our Lewis acidity scale based on fluoride affinities and have expanded our F+ affinity scale. These are being used to explain the reactivity of inorganic fluorides related to high energy materials.

We have developed an improved understanding at the molecular level of the atomic layer deposition of hafnium organometallics relevant to the generation of HfO2 surfaces on silicon for electronics applications

Contributions to Other Disciplines:

We have developed a new approach to the design of very sensitive sensors. The sensitive and selective sensors developed as part of this project will benefit the national economy, improve energy and national security, and be useful in environmental applications. Such sensors have potential applications in the areas of health, biomedical, and law enforcement.

We have generated an improved understanding of the properties of Nitinol alloys for aerospace applications.

Contributions to Human Resource Development:

We have introduced the idea of using computational chemistry to solve important problems in nanoscience at the undergraduate level. This is being done by engaging students in the University of Alabama Computer Based Honors Program in such studies. We have had a significant number of female undergraduate students working on this and related research projects. They have made significant contributions and have presented their work at a number of university and university-system sponsored research conferences. In addition, they have been involved in peer-reviewed publications. It is important to get undergraduates involved in research to get them to consider careers in science. We also published a paper in the Journal of Physical Chemistry with a female graduate student from Mexico who visited us for 3 months to work with us on this project.

The Dixon group sponsored 6 REU students (2 women) from non REU funding during the summer of 2010. The Dixon group had 9 undergraduate students (1 woman) in the Fall 2010 and Spring 2011 semesters. Two undergraduates (1 woman) won two of the 3 upper level UA Chemistry Department Awards. Two students (1 woman) were named Goldwater Scholars. Five of the 15 Randall Undergraduate Research Awards were awarded to students working in the Dixon group including 3 women and one student was awarded the Pettus Randall Scholarship for outstanding research by a student in the Computer Based Honors Program at UA. Two undergraduate students graduated from the group in Spring 2011 and both are in medical school at The University of Alabama-Birmingham.

The Gole group has 6 undergraduate researchers, 2 of whom are women.

Contributions to Resources for Research and Education:

We are currently using the research advances in this area in our undergraduate Physical Chemistry Laboratory and Honors Freshman Chemistry Laboratory. We are also incorporating results from our work into the Freshman Learning Community seminar courses at The University of Alabama. We are involving undergraduate students in research that leads to publications in peer-reviewed journals. We will incorporate ideas about the inverse hard and soft acid base coupled with semiconductor physics model into our courses in terms of molecular properties and the design of real systems.

Contributions Beyond Science and Engineering:

Conference Proceedings

Categories for which nothing is reported:

Any Web/Internet Site

Any Product

Contributions: To Any Beyond Science and Engineering
Any Conference

NIRT: Active Nanoparticles in Nanostructured Materials Enabling Advances in Renewable Energy and Environmental Remediation

Annual Report, May, 2008

Overview

Our research efforts during this period have involved a combined experimental and computational effort to characterize the behavior of active nanostructures. We have been concerned with the formation and study of unique porous silicon interfaces, the characterization of uniquely doped and modified TiO_2 nanostructures, and the characterization of silica nanostructures. A major focus has been to study porous silicon (PS) interfaces in order to (1) produce the first high temperature photocatalytically active microfilters, (2) evaluate the mass transport inherent to PS microreactor and sensor configurations, and (3) produce nanostructure modified PS microreactors leading to efficient photocatalysis, using both solar and electroluminescence based optical pumping, and (4) produce selective sensor interfaces.

During this period, we have further developed techniques to produce highly doped (metal, metal oxide, and metal-water complexes) TiO_2 and $TiO_{2-x}N_x$ thin and thick films that not only can be made photocatalytic but also display novel behavior with respect to the nature of the temperature dependent transformation of the anatase to the rutile phase of titanium dioxide. These results for TiO_2 nanostructures smaller than 40 nm are important not only for photocatalysis but also for the sintering process and the formation of nanostructured ceramics. Within the framework of PS microreactors, having completed the first phase of elevated temperature operative nanostructure coated microstructure-based filter development, we are continuing to seed microfilters with active nanostructures to form the basis of a flow through reactor configuration that will complement the photoluminescence and electroluminescence-based microreactors we are developing.

We have now developed novel TiO_2 nitrogen doping ($TiO_{2-x}N_x$) and metal ion seeding techniques leading to the discovery of (1) novel room temperature anatase to rutile phase transformations, in contrast to the usual high temperatures needed for the transformation, (2) magnetic ion (Fe^{II}, Co^{II}, Ni^{II}) enhanced Raman and enhanced infrared spectroscopy of the oxynitride, and (3) magnetic ion enhanced nitrogen doping. Further, we are now studying the apparent effects of nitrogen fixation observed for the Fe^{II} seeded oxynitride systems. Finally, following the studies outlined above we have observed the unexpected hydrophobic character introduced to transition metal-ion-water complexes seeded into TiO_2 or $TiO_{2-x}N_x$. With the intent of preparing appropriate active nanostructure support systems and following our previous studies, we are engaged in a study of silica-based nanostructures, Si_xO_y, in which the transformation from hydrophilic (SiO_2) to hydrophobic character can be induced with syntheses based on an increased Si/O ratio.

Thin and Thick Film Photocatalytic Surfaces and Phase Transformation at the Nanoscale

A major portion of our work has focused on the characterization and processing of titanium dioxide (TiO_2) thin films from the synthesis stage, with special attention paid to microstructure

phase transformation, and alternative doping methods. These two areas are of critical importance to the formation of TiO_2 based systems. For example, the phase of TiO_2 is intrinsic to its surface-adsorbate and bulk carrier transport characteristics, whereas dopant incorporation is critical to lowering the band gap energy to enhance quantum efficiency and solar photon conversion, especially for photochemical water splitting.

The phase transformations of TiO_2 films and nanoparticles are governed by their synthesis and preparation procedures in ways that are not yet fully understood. Synthesis parameters such as annealing temperature, annealing atmosphere, etc., have shown dramatic effects on the transformation behavior of those particles that are obtained. The studies that we reported previously on a variety of surfaces demonstrated the importance of clarifying the interaction with the various surfaces on which TiO_2 or $TiO_{2-x}N_x$ is formed as a film. Interactions with the phonon modes of the surface may give rise to anatase to rutile phase transformations at temperatures well below that required for the stoichiometric conversion of TiO_2. The driving force of these phase transformations can also be altered from thermodynamic to dominantly kinetic in nature.

We have continued to study of the heat treatment induced particle agglomeration and phase transformation for these titania (TiO_2) nanoparticles. Recent work has shown that the use of combinations of the two major phases (anatase and rutile) provides distinct benefits in both photocatalytic activity, as well as increasing the effective absorption wavelength. For this reason we have been interested in controlling very precisely the phase transformation percentage in agglomerated TiO_2 nanoparticles. These studies were carried out on only TiO_2 nanoparticles over the temperature range extending from room temperature to in excess of 800ºC where the anatase to rutile conversion typically is found to occur. Results obtained for both a porous sol-gel-generated nanocolloid (3-20 nm) and a sol-gel-generated micelle nanostructure (~ 40 nm) were evaluated. While the TiO_2 nanocolloid structures aggregate to form larger crystallites as a function of increasing temperature with sizes comparable to the sol-gel-generated micelle structures, the resulting *anatase crystallites, which are of a diameter 40-50 nm, appear to transform to comparable or slightly smaller rutile structures at 800ºC.* This is in contrast to the transformation to larger rutile structures, observed for larger nonporous anatase particles. These results are significant not only for the formation of anatase/rutile co-phase production at temperatures slightly below that for the complete conversion of the anatase to the rutile phase, but also to the sintering process and to the formation of nanostructured ceramics. Kinetic effects are considered to be of greater importance at the nanoscale as they enhance the rate of anatase to rutile conversion. These characteristics have been established using a combination of Raman spectroscopy, X-ray diffraction, and scanning electron microscopy. The relative playoffs of Raman and X-ray diffraction techniques have been considered as they are used for the analysis of particles at the nanoscale, especially when phase transformations are evaluated. In our studies we have found that Raman spectroscopy provides distinct benefits as compared to the more widespread use of X-ray diffraction studies (XRD). The use of Raman spectroscopy provides easily visualized data on the extent of phase transformation (characteristic vibration spectra), as well as the effective size of nanoparticles (line-width of the vibrational peaks). Our experiments demonstrated that during phase transformation the anatase particles condensed to form smaller rutile particles (the density of a rutile particle is somewhat greater than that for anatase). To ensure the accuracy of our work, we compared this to XRD data for the same powders, and the

results were markedly different. The XRD spectra suggested an increase in particle size during transformation, in direct opposition to the Raman results.

To solve this discrepancy we employed Scanning Electron Microscopy and determined that the Raman result was indeed correct. Therefore the calculation of particle size using the Debye-Scherer equation to study phase transformations can lead to erroneous results. The Debye-Scherer equation relates particle size to the broadening of an X-ray diffraction peak. This however does not take into account the disordering of agglomerations of particles that may occurs during transformation. For example, it is believed that anatase titanium dioxide particles undergoing transformation to the rutile phase show a large increase in disorder because of the shift from end-on octahedra (anatase) to side-on octahedra (rutile) configuration. We have shown that the results of the direct use of the Debye-Scherer equation in situations such as this are improper. Because the Raman technique is not geometrically constrained, the disordering during phase transformation does not affect the calculation of particle size. This work has been submitted for publication in the *Journal of Physics and Chemistry of Solids*.

Besides material characterization and preparation, we also are developing applications, and we have been involved in the design and fabrication of a suitable test reactor (Figure 1) for the determination of the reaction mechanism for hydrogen production from the photochemical splitting of water. The test reactor will be finalized and subsequently fabricated in the coming months using thin and thick films and surfaces fabricated from interfacial anatase/rutile nanostructured combinations and the metal, metal ion, and metal oxide doped TiO_2 and $TiO_{2-x}N_x$ nanostructured materials (see following) that we have now developed in our laboratory. With the fabrication of this reactor, we will begin to study the intrinsic surface kinetic mechanisms of hydrogen production from water. Specific goals are to provide cheap hydrogen production at a fraction of the cost of silicon-germanium solar cells and electrolysis systems.

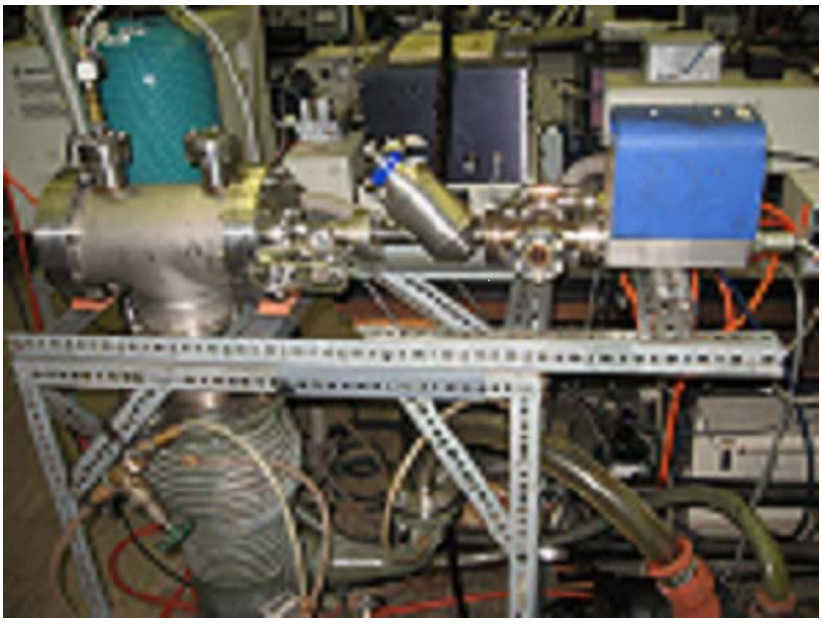

Figure 1: Apparatus for the study of water formation from seeded titanium dioxide.

Nitrogen Doped and Metal Ion Seeded TiO_2

We have continued to investigate the influence of nitrogen dopant concentration on the electronic structure tuning and photocatalytic activity of porous $TiO_{2-x}N_x$ nanoparticles. We have now conducted a series of studies with a basis to evaluate the relative and cumulative effect of high spin Co^{II}, Ni^{II}, and Fe^{II} ions, introduced as the metal halide and metal nitrate hydrate vs. the low-spin Cu^{II} ion. In addition, we have studied the self-assembly of the silver clustered oxides in TiO_2. These studies have lead to several unique observations at elevated metal ion seeding which suggest that novel simultaneous metal atom and ion-based seeding and nitrogen doping can produce uniquely active nanostructures.

We have investigated the efficient room temperature conversion of anatase to rutile TiO_2 induced by high spin ion doping. The surprising room temperature phase conversion of anatase to rutile TiO_2, a process that normally requires temperatures well in excess of 700ºC, has been found to be facilitated through the use of transition metal ions with highly unpaired electron spin. Raman spectroscopy has been used to demonstrate this unexpected process, facilitated through the use of high spin cobalt (Co^{II}) and nickel (Ni^{II}) transition metal ion seeding into a TiO_2 or $TiO_{2-x}N_x$ nanocolloid lattice. In distinct contrast, the effect is not manifest upon seeding with low spin ions including Cu^{II}. The Raman spectra also demonstrate the concomitant incorporation of a spinel-like structure into the titania lattice that we suggest influences the high spin cobalt interaction.

We have carried out a comparative study of the simultaneous Co^{II} ion seeding of TiO_2 and $TiO_{2-x}N_x$. Experiments with a porous sol-gel-generated TiO_2 nanocolloid and its corresponding oxynitride $TiO_{2-x}N_x$ are extended to evaluate the cumulative effect of further doping with the high electron spin cobalt (Co^{II}) ion. A combination of Core and VB Photoelectron spectroscopies complement the data obtained with Raman spectroscopy to demonstrate that porous sol-gel-generated anatase TiO_2 and nitridated $TiO_{2-x}N_x$ can be simultaneously doped with metallic cobalt (Co^{II}) ions to introduce a cobalt oxide-based spinel-like structure into both the TiO_2 and nitrogen doped $TiO_{2-x}N_x$ lattice. The VB Photoelectron spectra also demonstrate that cobalt cluster formation is negligible although the Co^{II} concentrations considerably exceed those used by previous workers. The formation of these metal ion doped titanium oxide based surfaces introduces a significant hydrophobic character to the hydrophilic cobalt chloride complexes used in this study. The creation of a spinel-like structure is commensurate with the room temperature conversion of the oxide and its oxynitride from the anatase to the rutile form. While this phase conversion is also observed in preliminary studies of Ni^{II} ion doping, we have found that it does not occur for the Cu^{II} ion.

We have obtained evidence for high spin transition metal ion induced infrared spectral enhancement. Using the cobalt (Co^{II}) and nickel (Ni^{II}) ion seeding of a nitrogen doped titanium oxynitride, $TiO_{2-x}N_x$, we have demonstrated a significant enhancement of the infrared spectrum associated with adventitious water and minor contaminants associated with the oxynitride synthesis from a porous TiO_2 nanocolloid sample. We suggest that this infrared enhancement is associated with the formation of protonated amines near the oxynitride surface. The intensity enhancement also may be associated, in part, with the modification of the anatase ionic crystal dipole moment due to the displacement of charged ions by the electric field, which is associated

with the introduced high spin Co^{II} and Ni^{II} ions. The concomitant incorporation of a spinel-like structure into the TiO_2 lattice as suggested by our Raman spectroscopic studies may account, in part, for the enhancement.

We have demonstrated diffusion controlled self-assembly and dendrite formation in silver seeded anatase titania nanospheres. We have studied the diffusion-controlled, solvent-mediated self-assembly and dendritic structure formation as anatase TiO_2 is seeded with the silver oxides and silver formed using silver nitrate (zinc-catalyzed). Anatase TiO_2 nanocolloid solutions have been seeded with silver nitrate over a concentration range extending to saturation as the zinc-catalyzed transformation of the nitrate is studied in a number of solvents used in the formation and study of porous silicon interfaces. In acetone alone and, to a lesser extent, butanone, the silver/silver-oxide seeded titania nanoparticles assemble into needle-like arrays of significant extent. This assembly is greatly accentuated in benzene/acetone mixtures, and to a much lesser extent in diethyl ether/acetone mixtures, due primarily to the significant vapor pressure of the ether. In contrast to these aprotic solvents, self-assembly cannot be induced in the protic solvents water, methanol, and ethanol, or in the aprotic solvents acetonitrile, methylene chloride, and dimethylformamide, even in mixtures with acetone. These results are explained and attributed to several controlling factors: the titania crystal structure and the nature of its subsequent silver seeding; the nature of diffusion through the considered solvents; the formation of silver acetate, propionate, and benzoate; and the formation of strong cyano and chloride bonds. At saturated silver nitrate concentrations, distinctly different solvent-mediated dendrite growth in water and acetone solvents is explained from the perspective of a diffusion limited aggregation (DLA) process.

Deposition of TiO_2 nanoparticles onto nickel surfaces and nanoparticle reactivity

Over the past year we have developed a means to uniformly deposit chemically synthesized TiO_2 based nanoparticles from solution onto a Ni foil so that we can do ultra-high vacuum surface science studies on such materials. This is an important technical success for three reasons: (1) the "film" of nanoparticles does not charge under photoemission experiments, (2) the Ni film can be resistively heated in a highly controlled manner for thermal desorption experiments, and (3) the uniform coating ensures that no adsorption occurs on the Ni substrate. Our focus has been to understand the thermal and photochemistry of simple molecules, namely H_2O, O_2, and CH_3OH, on ~1% nitrogen doped TiO_2. The thermal desorption spectra of these molecules produce a peak desorption temperature for 1 monolayer that is similar to slightly defective TiO_2 single crystals. However, there is a considerable high temperature tail which suggests that there are more defects in the nanomaterials.

To better understand the role of the electronic structure of N-doped TiO_2 on photon-driven reactions, we irradiated 1 monolayer of molecular oxygen and methanol at ~ 105 K (using a low pressure Hg arc source and filter) with greater than ~ 365 nm photons. Since both O_2 and CH_3OH are known to be hole-scavenging molecules, they are a sensitive probe of the electron-hole recombination dynamics. Post-irradiation temperature programmed desorption (TPD) indicated a very low quantum yield for O_2 photodesorption compared to TiO_2 single crystals, which suggests the N doped TiO_2 nanoparticles contain more defects that serve to trap the photoexcited carriers. Over the next year we plan to prepare less defective nanoparticles by

optimizing the post-synthesis annealing temperature, time and ambient gas environment. Also we plan to study of the effect of particle size and nitrogen concentration on the wavelength dependent photochemistry of adsorbates.

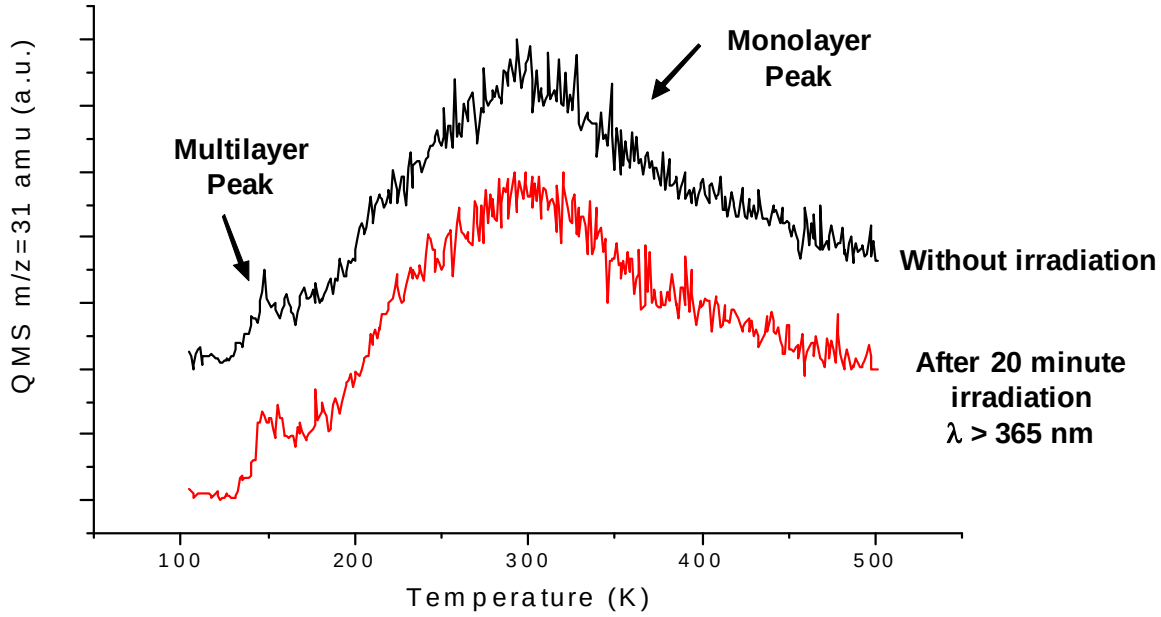

Figure 2. Temperature programmed desorption of CH3OH (3 L dose)

Modeling Porous Silicon as a Photocatalytic Reactor Support Structure

Interest in using porous silicon for catalytic reactors is motivated by its high accessible surface area (per unit volume), which is a result of its open branching-porous morphology. It has also been found that porous silicon's electrical properties (e.g., electrical impedance) change as a result of the introduction and adsorption of different chemicals to the PS surface. These characteristics of porous silicon, such as (i) electrical and luminous property variation in response to the presence of specific chemical species, (ii) the promise of manufacturing simplicity, and (iii) good sensitivity (as a result of a high surface area to volume ratio), make it a potentially useful substrate material for chemical sensing and reaction devices.

As is the case for all chemical reactors and sensors, the response of porous silicon reactors is generated upon interaction of a target chemical (analyte species *A*) with the chemical recognition interface, either the silicon surface or another material intimately coupled to the silicon. This interaction occurs in nanopores of the PS reactor, and is often facilitated by the presence of a metal or metal oxide. In a recently published book chapter, we reviewed transport processes underlying the transient response of PS chemical reactors and to provide theoretical tools which will facilitate the formulation of mathematical models of porous silicon reactors. The resulting first principles models consist of governing mass transfer equations which can be solved analytically in some cases, or for more complex configurations and with sufficient computing resources, can be solved through numerical simulations. A motivation for formulating such

models is that, at present, both the interpretation of results and design of PS reactors are in some respects empirical. A notable advantage obtained through the use of a first principles model is that calibration becomes a measurement of transport properties and surface kinetics parameters, in addition to the properties inherent to the relevant reaction mechanism. A secondary purpose of the chapter was to demonstrate routes to further simplification so that *analytical* or at least *semi-analytical* solutions to the mass transport model may be possible. In general, the solution of a mathematical model of the transport-reaction system is too complex and can only be accomplished numerically, using, for instance, finite volume, finite element, or finite difference techniques, implemented through either commercially available or user-written computer codes. When using numerical simulation, for any given combination of input parameters and sensed species concentrations, only a single prediction of the resulting reactor output is obtained. The resulting parametric space, even after non-dimensionalization, is large; filling this space is time consuming and tedious so extracting useful insight from the results is difficult. To be useful to practitioners, a theoretical tool must be accurate yet simple enough not to require special skills for implementation, and it must be expressed in terms of meaningful and accessible physical parameters. Analytical solutions are therefore very useful and complement numerical simulations by providing additional insight so it is often worth introducing carefully validated simplifications in the model to obtain them. We demonstrated the application of such analytical approaches in this chapter in detail.

Modification of the Active Porous Silicon Interface

On the basis of low resistance contacts to a PS interface, we propose to develop microreactors in which visible light absorbing quantum dot (QD) photocatalysts are placed within the pores of PS and excited using PS electroluminescence or photoluminescence. Highly efficient light absorbing titania-based nanocolloids, produced in a nanoscale exclusive synthesis at room temperature, can be nitridated in seconds to produce nitrogen doped, stable, and environmentally benign $TiO_{2-x}N_x$ photocatalysts whose optical response can be tuned across the entire visible region. Tunability throughout the visible is found to depend upon the degree of nanoparticle agglomeration and upon the ready ability to seed the nanoparticles with metals (metal ions) and additional active particles. These photocatalysts readily photodegrade methylene blue and gaseous ethylene. It is significant that these oxynitride ($TiO_{2-x}N_x$) quantum dots can be transformed from liquids to gels, and, in addition, can be placed on the PS surface in a sensor or microreactor based conformation to produce an improved photocatalytically induced solar based sensor or microreactor response. Films constructed from colloidal solutions of $TiO_{2-x}N_x$ and Pd- $TiO_{2-x}N_x$ on a quartz surface are photocatalytically active for the total oxidation of ethylene to carbon dioxide under UV and incandescent light illumination at room temperature. The nitriding procedures we have employed can produce surface based doped titania photocatalyst centers which are catalytically active within a broad range of optical excitation well into the visible range. These results provide strong evidence that novel materials which can be synthesized at room temperature can be conveniently used to coat silicon-based surfaces to produce, under visible light illumination, strongly oxidizing photocatalytic centers. The strategy of such an effort should be to generate uniquely optimized photocatalytic films by modifying the nature of those centers that produce the photocatalytic activity. An effort with this goal is now underway in our laboratory. In recent experiments (Figure 3) we have now successfully deposited TiO_2 and $TiO_{2-x}N_x$ nanoparticles to the PS framework. This effort has yielded an

~60% coverage at the present time and shows considerable promise. We are now working on means to strongly activate these and the additional unique titanium-oxide-based nitrogen and metal doped systems we have generated in our laboratory.

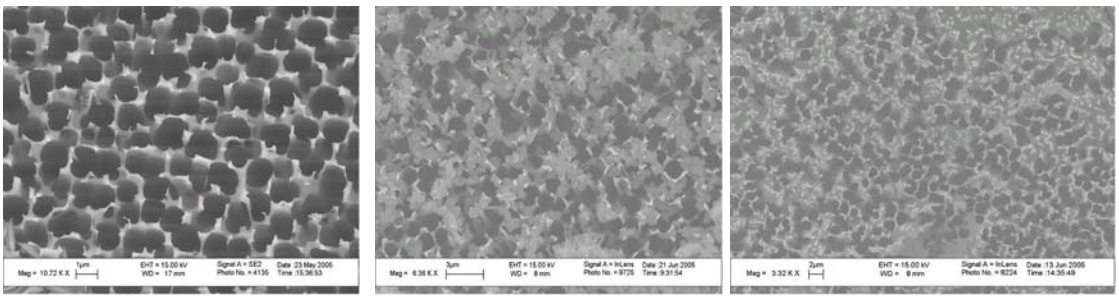

Figure 3. (a) Closeup top view of hybrid porous silicon films. (b) 100-200nm TiO_2 nano particles coating on porous silicon micropores; (c) 10nm $TiO_{2-x}N_x$ nano particles coating (60%) on porous silicon micropores.

Development of Porous-Silicon-Based Active Microfilters

We have now readily produced micro/nanoporous silicon film which serves as an inorganic (vs. polymer) filter, using a very specific etch procedure (Figure 4) which has now been published in the *Journal of the Electrochemical Society*. With a goal of preparing silicon-based interactive filters in the micropore range, we have developed the first single-step etch-liftoff procedure (one-step separation) based on the formation and removal of macroporous silicon layers (Figure 5). With silicon wafers whose resistivities are in the range from 14 to 22 Ω cm, we are able to create, in a surprisingly controlled manner, films whose pore diameters range from 1-2 μm and whose thickness ranges from 3 to 70 μm. These silicon-based films (filters), which carry a polarizing negative charge, represent an alternative to porous alumina (files) filters (pore diameter not yet in the 1-2 μm range) both in terms of their size range and potential interaction-reaction at elevated temperature. Preliminary experiments demonstrate that platinum and copper can be introduced into these filters using electroless solutions with a goal to creating an effective reductive surface. Using these and alternate material combinations, interactive-reactive filters in the 1 μm size range that operate at temperatures well in excess of porous polymer films can be realized. We are continuing our development of these active microfilters using subsequent treatments with additional active nanostructures to form flow through microreacters.

Behavior of Nanostructured Silicon Support Surfaces

Silica support surfaced are known to play an important role in catalysis. Recent studies in our laboratory of the activity of silica nanospheres and their comparison to Cab-O-Sil® have suggested the importance of the silicon oxides, Si_xO_y,as active nanostructures. We now have carried out a study in which we have analyzed the surprising oxidation state of fumed silicon and the nature of water binding to the silicon oxides and hydroxides. Here, we analyze arresting X-ray photoelectron spectroscopy (XPS) data that demonstrates that the average formal oxidation state of silicon in fumed silica (Cab-O-Sil®) is +1 as opposed to the previously envisioned +4. In concert with electronic structure calculations on model molecular clusters, the results suggest a notably more hydrophobic character for Cab-O-Sil® that the oxides of silicon with Si in the

formal +3 and +4 oxidation states. The nature of the fumed silica oxidation state and the determined notable changes in the nature of water binding to the +1 to +4 oxidation states have important implications for the expanded use of silica-based materials. We are currently extending this work to study the activity of shifting nanoscale silicon oxide oxidation state distributions where we demonstrate the transition from hydrophilicity to hydrophobicity with increasing average Si/O ratio.

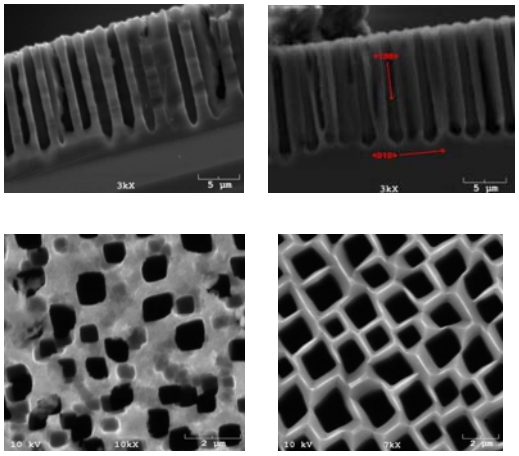

Figure 4: SEM micro-graphs of a porous silicon filter. In the top images, the tips of the pores can be seen before (left) and after (right) they begin to spread out in their face directions. The bottom images show the front (left) and back (right) of a filter. Note that pore spreading is significant in the filter back.

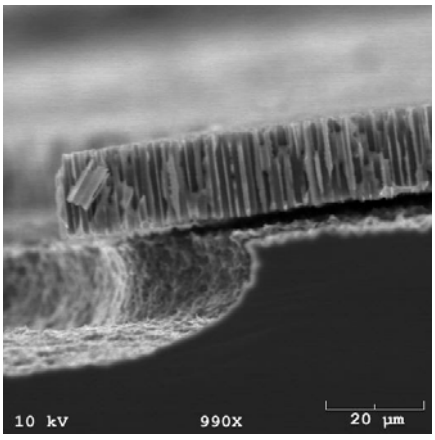

Figure 5. Direct Lift-off of PS-based film- filter (~ 20 microns) from the surface of an etched PS film. Pore diameter is approximately one micron

Molecular Structures and Energetics of the $(TiO_2)_n$ (n = 1−4) Clusters and Their Anions

TiO_2 with band gaps of 3.0 eV for rutile and 3.2 eV for anatase is an active photocatalyst as well as an important catalyst support. We have been exploring the properties of TiO_2 nanoclusters. The $(TiO_2)_n$ clusters and their anions for n = 1−4 have been studied with CCSD(T) and DFT. For n > 1, numerous conformations are located for both the neutral and anionic clusters, and their relative energies were calculated. The CCSD(T) energies were extrapolated to the complete basis set limit for the monomer and dimer, and calculated up to the triple zeta level for the trimer and tetramer. The ADEs and VDEs of the anionic clusters to the ground and first excited states of the neutral clusters were calculated and compared with the experimental results to provide definitive assignment of the ground state structures of the anionic clusters. Anions of the dimer and tetramer are found to have very closely-lying conformations within 2 kcal/mol at the CCSD(T) level, whereas the trimer anion does not. Accurate clustering energies and heats of formation were calculated for the neutral clusters and compared with the available experimental data. Estimates of the titanium-oxygen bond energies show that they are stronger than the group VIB transition metal-oxygen bonds except for tungsten. The atomization energies of these clusters display much stronger basis set dependence than the clustering energies. Use of the clustering energies enables the calculation of more accurate heats of formation for larger clusters.

This allows the calculation of more accurate heats of formation for larger clusters on the basis of calculated clustering energies and represents a novel approach to the prediction of heats of formation of transition metal containing molecules and nanoclusters. The energies of these structures are also being calculated at the density functional theory (DFT) level for a wide range of functionals (~25) to benchmark DFT.

Our CCSD(T) and DFT calculations show that the first excitation energy gaps exhibit a strong dependence on the cluster structures. Figure 6 displays the adiabatic energy gaps (the energy differences between the first triplet excited states and the ground states of the neutral clusters) at the CCSD(T)/aD// B3LYP/aD level. The first singlet and triplet excited states of these clusters are energetically nearly degenerate so these adiabatic energy gaps are good approximations to the first singlet excitation energies for the cluster. These gaps, except for the tetramer are below the band gap of the bulk material and show that controlling the particle size and structure will be important in controlling the photocatalytic activity of TiO_2 nanoparticles. The energies of the ground state of the low-lying conformations lie within ~15 kcal/mol at the CCSD(T) level to the ground states of these clusters. Thus, they may be present on the surface of TiO_2 catalysts, depending on the manufacturing process, the support, and other environmental effects. This could be a reason for the strong dependence of the photocatalytic activity of titanium dioxide particles on the manufacturing process. As there are a number of low-lying structures with distinct energy gaps, one should be able to tune the photocatalytic properties of the titanium dioxide particles by varying the size and structural distribution with different preparation

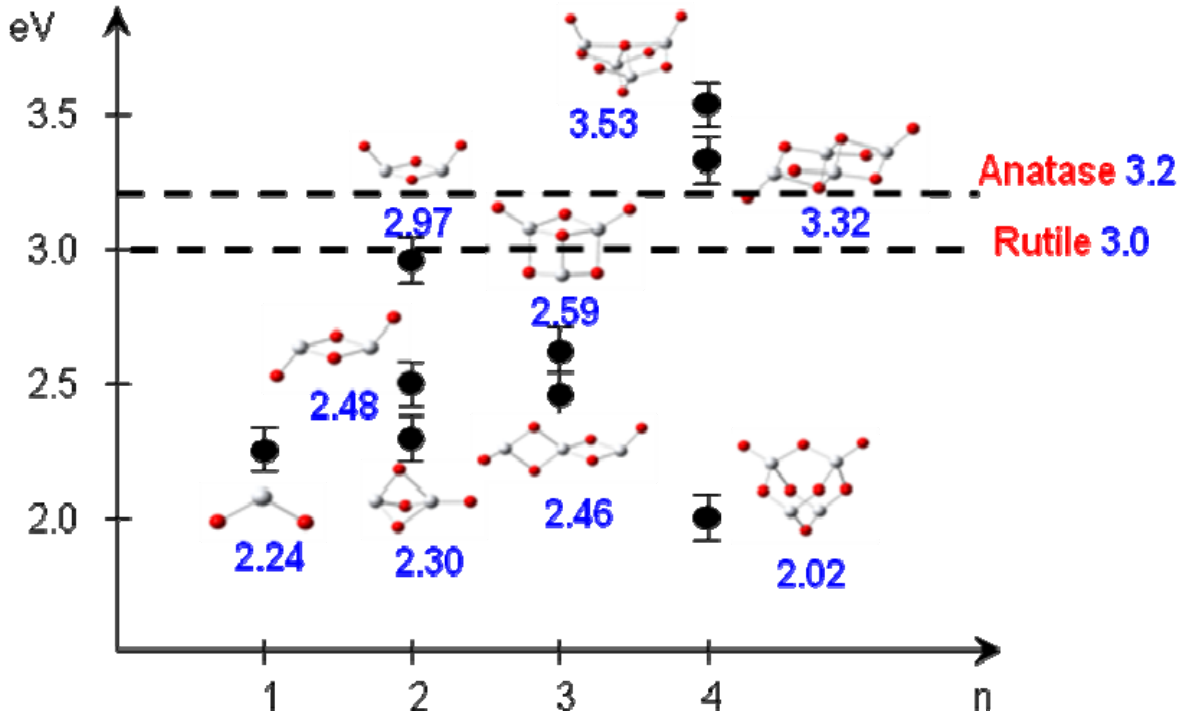

Figure 6. Adiabatic energy gaps for the low-lying structures of the $(TiO_2)_n$ (n = 1−4) clusters calculated at the CCSD(T)/aD//B3LYP/aD level relative to those of the bulk values.

methods and/or different supports. An important feature is that the band gap of the cluster can be tuned to be more in the visible region so that the TiO_2 particles can more efficiently absorb solar

radiation at the Earth's surface. The extra electron in the anion is localized on a single metal center for the monomer and trimer, but is partially delocalized on two Ti centers for the dimer and tetramer. In most cases, the extra electron in the anion is localized in the Ti $3dz^2$ orbitals except for the monomer and certain structures of the tetramer where other d orbitals are involved. The anions contain electron-rich titanium center(s) with strong electron donating capability. These anions are expected to be very reactive, which may contribute to the photocatalytic activity of titanium dioxide.

Experimental and Theoretical Studies of the Photoreduction of Metal Ion-Dendrimer Complexes: Observation of a Delocalized Organic Radical

Metal dendrimer nanocomposites were prepared by ultraviolet (UV) irradiation of Cu(II) or Zn(II) dendrimer solutions. Organic free radicals were detected in the metal ion dendrimer solutions by EPR experiments following UV irradiation. Spectral simulations and quantum chemical calculations were carried out to elucidate the nature of the free radicals. The free radicals produced were found to be dendrimer radical cations. Both spectral simulations and electronic structure calculations suggest the electron spin density to be localized on the central N-C-C-N core structure and delocalized over the N and C atoms in the core. The radical cations of model structures with the ethylenediamine (EDA) core and that of the G0-NH2 polyamidoamine (PAMAM) were found to have a weak central one-electron C-C bond. The description of the molecular structure of the cation falls between the limit of two iminium-type ions with a charge of +0.5 e on each ($^{½+}R_2N{=}CH_2{}^{½\bullet}$) interacting by a one electron C-C bond and the other limit of a $^{½+½\bullet}NR_2\text{-}CH_2\text{-}CH_2\text{-}NR_2{}^{½+½\bullet}$ structure with a spin of 1/2 and a charge of 1/2 on each N. For EDA, our calculated ionization energies and heats of formation at the coupled cluster (CCSD(T)) level are in good agreement with available experimental data. The ionization energy of the G0-NH_2 PAMAM was found to be substantially lower than that of EDA. The reduction in the ionization energies for the dendrimers and other effects such as metal-ligand interaction and solvation contribute to the reduction of metal cations by dendrimers with UV irradiation. Similar experiments with the G0-NH_2 poly(propylene imine) (PPI) did not produce metal nanoparticles, indicating these effects are not as favorable as for G0-NH_2 PAMAM. Figure 7 shows the relationship between the number of electrons in a carbon-carbon bond and the bond length for these cations calculated at the B3LYP/DZVP2 level, compared with those for $CH_3{-}CH_3$, $CH_2{=}CH_2$, and CH≡CH. There is an approximate linear relationship between these two quantities, suggesting that the number of electrons in the internal C−C bond is ~0 for the cation of EDA, and ~1 for the cations of TMEDA, TEEDA, and G0-NH_2 PAMAM. Obviously, there is electron density between the two C atoms in the EDA cation but it is not large. In order to provide more insight into the relationship between the BDEs and the number of electrons in the bond(s) between two carbon atoms, we plot the BDEs in Figure 7 for EDA^+, $TMEDA^+$, C_2H_6, C_2H_4, and C_2H_2. The plot is approximately linear again and the one electron BDEs fall on the linear plot, suggesting that they really are one electron bonds. This conclusion differs from that derived from the bond length plot in that EDA+ has a one electron bond suggesting that the BDEs are a more sensitive measure of the number of electrons in the bond. This is also consistent with the result that the one-electron BDEs exhibit very little dependence on substituents whereas the bond distance has a significant dependence on the substituents.

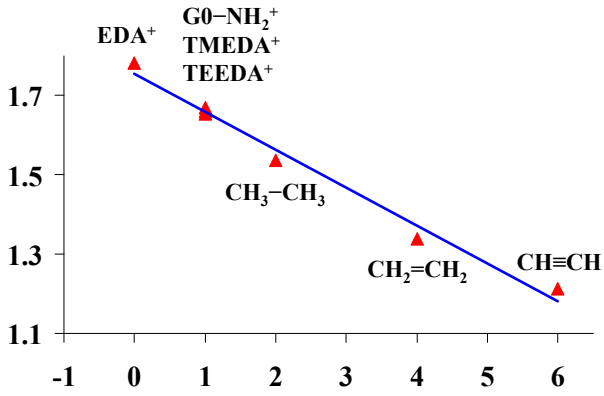

Figure 7. The carbon-carbon bond length in Å plotted against the number of electron shared by the carbon atoms, showing a linear relationship between these two quantities

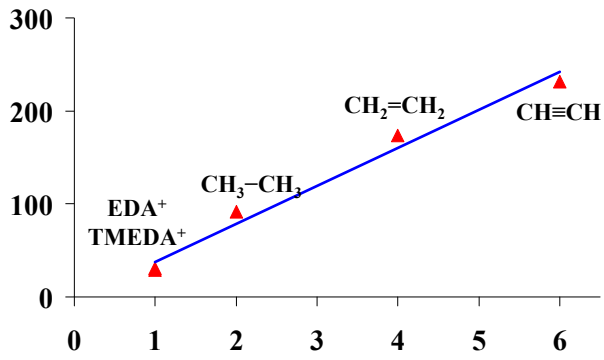

Figure 8. The carbon-carbon adiabatic BDEs in kcal/mol plotted against the number of electron shared by the carbon atoms, showing a linear relationship between these two quantities

Application of Photocatalysis for Sustainable Energy

Recently, we have begun to investigate a new use of photocatalysis for the synthesis of liquid fuels from a renewable energy source using water and carbon dioxide as a feedstock. Several investigators have sought to solve the coming hydrogen storage problem by the direct photocatalytic reformation of carbon dioxide (CO_2) impregnated in liquid water in order to form high energy density liquid fuels such as methanol. Because of the low solubility of CO_2 in water (23 PPM at standard conditions) we suggest that this method is not viable from an industrial point of view. To overcome the CO_2-water solubility limitation, we have begun an investigation into an indirect method of reformation of CO_2 and water into the high value liquid fuel methanol. We have chosen methanol for our fuel as its manufacture is a well established, high energy efficiency process which is well suited to industrial production. We have assembled a high pressure reaction vessel to voltammetrically investigate the redox potential of high pressure liquefied CO_2. We intend to generate both hydrogen (H_2) and carbon monoxide (CO) through separate photocatalytic reactions. The process we are studying is the reformation of CO_2 into CO. One potential reaction mechanism for this process on TiO_2 is shown in Equations 1-3,

$$CO_2 + e^- \rightarrow CO_2^- \qquad (1)$$

$$CO_2^- + CO_2^- \rightarrow CO_3^{2-} + CO \qquad (2)$$

$$CO_3^{2-} + 2h^+ \rightarrow CO + O_2 \qquad (3)$$

where e^- is a photogenerated conduction band electron, h^+ is a photogenerated valence band hole, and CO_3^- is a radical carbonate intermediate. The multistep reaction listed in Equations 1-3 is only one of the several possibilities we intend to study using voltammetric methods. With this information, we aim to generate both of the precursors for methanol synthesis, thus establishing a renewable method of generating liquid fuels for mobile and distributed power production.

Bond energies for organic compounds bonding to TiO_2

There is substantial interest in the use of TiO_2 for the photocatalytic decomposition of ortganic compounds. There have been a number of experiments dealing with the photodecomposition of compounds derived from ketones. The ketones react with oxygen and the surface to generate

diolates. These diolates can then decompose under irradiation to form acetate type ions as shown in Figure 9. An interesting result arises when the groups bonded to the carbon differ, e.g. instead

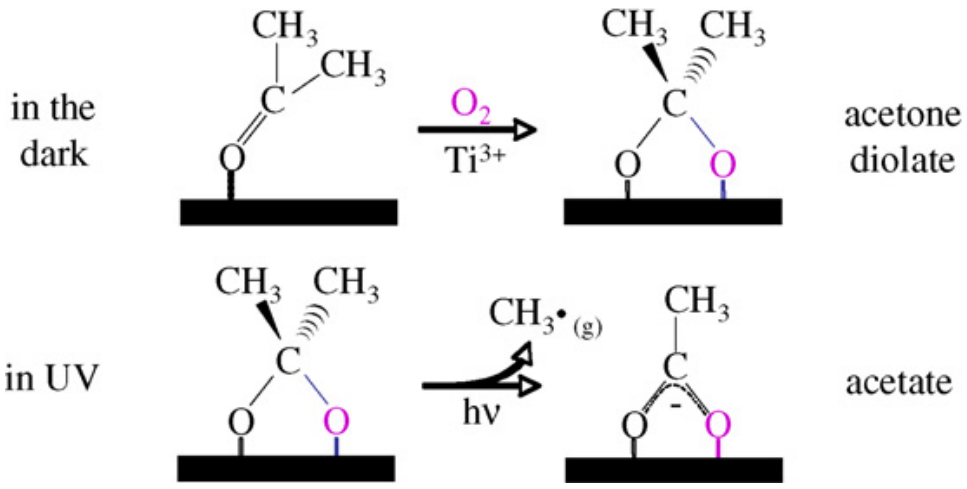

Figure 9. Schematic of bonding and reactivity of acetone on TiO_2. (from M.A. Henderson, J. Catalysis, in press, 2008, doi:10.1016/j.cat.2008.03020)

of two CH_3 groups, there is one CH_3 and one CF_3 group. Which group will come off on irradiation? We have modeled this process by looking at the adiabatic bond dissociation energies BDEs at the G3MP2 level (Table 1). The calculated BDEs are in general agreement with the temperature programmed desorption (TPD) studies of Henderson and show that the weakest bond breaks first. This was used to explain the experimental results and correct a misinterpretation of the observations.

Table 1. G3(MP2) Adiabatic C-X Bond Dissociation Energies at 0K in kcal/mol.

Bond energy reaction	**BDE**
$CH_2(OH)_2 \rightarrow CH(OH)_2 + H$	95.1
$CHCH_3(OH)_2 \rightarrow CH(OH)_2 + CH_3$	87.8
$CHCH_3(OH)_2 \rightarrow C(CH_3)(OH)_2 + H$	94.6
$C(CH_3)(C_2H_5)(OH)_2 \rightarrow C(C_2H_5)(OH)_2 + CH_3$	87.5
$C(CH_3)(C_2H_5)(OH)_2 \rightarrow C(CH_3)(OH)_2 + C_2H_5$	87.2
$C(CH_3)(CF_3)(OH)_2 \rightarrow C(CF_3)(OH)_2 + CH_3$	89.3
$C(CH_3)(CF_3)(OH)_2 \rightarrow C(CH_3)(OH)_2 + CF_3$	95.8
$C(C(CH_3)_3)(CH_3)(OH)_2 \rightarrow C(C(CH_3)_3)(OH)_2 + CH_3$	87.5
$C(C(CH_3)_3)(CH_3)(OH)_2 \rightarrow C(CH_3)(OH)_2 + C(CH_3)_3$	84.9
$C(C_6H_5)(CH_3)(OH)_2 \rightarrow C(C_6H_6)(OH)_2 + CH_3$	79.4
$C(C_6H_5)(CH_3)(OH)_2 \rightarrow C(CH_3)(OH)_2 + C_6H_5$	99.2

$FCCH_3(OH)_2 \rightarrow FC(OH)_2 + CH_3$	92.4
$FCCH_3(OH)_2 \rightarrow CCH_3(OH)_2 + F$	121.3
$ClCCH_3(OH)_2 \rightarrow ClC(OH)_2 + CH_3$	87.5
$ClCCH_3(OH)_2 \rightarrow CCH_3(OH)_2 + Cl$	83.0
$CNCCH_3(OH)_2 \rightarrow CNC(OH)_2 + CH_3$	83.1
$CNCCH_3(OH)_2 \rightarrow CCH_3(OH)_2 + CN$	112.0
$NO_2CCH_3(OH)_2 \rightarrow NO_2C(OH)_2 + CH_3$	84.9
$NO_2CCH_3(OH)_2 \rightarrow CCH_3(OH)_2 + NO_2$	60.8
$CH_3CH_2CH_2CCH_3(OH)_2 \rightarrow CH_3CH_2CH_2C(OH)_2 + CH_3$	87.4
$CH_3CH_2CH_2CCH_3(OH)_2 \rightarrow CCH_3(OH)_2 + CH_3CH_2CH_2$	87.7
$CH(CH_3)_2CCH_3(OH)_2 \rightarrow CH(CH_3)_2C(OH)_2 + CH_3$	80.0
$CH(CH_3)_2CCH_3(OH)_2 \rightarrow C(CH_3)(OH)_2 + CH(CH_3)_2$	86.5
$CH_3CH_2CH_2CH_2CCH_3(OH)_2 \rightarrow CH_3CH_2CH_2CH_2C(OH)_2 + CH_3$	87.5
$CH_3CH_2CH_2CH_2CCH_3(OH)_2 \rightarrow CCH_3(OH)_2 + CH_3CH_2CH_2CH_2$	82.2
$CH(CH_3)(CH_2CH_3)CCH_3(OH)_2 \rightarrow CH(CH_3)(CH_2CH_3)C(OH)_2 + CH_3$	87.9
$CH(CH_3)(CH_2CH_3)CCH_3(OH)_2 \rightarrow C(CH_3)(OH)_2 + CH_3CH(CH_2CH_3)$	84.9
$CH(CH_3)_2CH_2CCH_3(OH)_2 \rightarrow CH(CH_3)_2CH_2C(OH)_2 + CH_3$	86.3
$CH(CH_3)_2CH_2CCH_3(OH)_2 \rightarrow CCH_3(OH)_2 + CH(CH_3)_2CH_2$	86.4

We are also studying the Brønsted and Lewis acidities of these compounds as represented by the OH^- affinity and are correlating these values (Tables 2 and 3) with the photoreactivity studies.

Table 2. G3(MP2) Brønsted acidities (ΔH for $AH \rightarrow A^- + H^+$) in kcal/mol at 298 K

Molecule	**Brønsted Acidity**
$CH_2(OH)_2$	368.1
$CHCH_3(OH)_2$	366.3
$C(CH_3)(C_2H_5)(OH)_2$	364.3
$C(CH_3)(CF_3)(OH)_2$	349.5
$C(C(CH_3)_3)(CH_3)(OH)_2$	361.7
$C(C_6H_5)(CH_3)(OH)_2$	354.9
$FCCH_3(OH)_2$	349.2
$ClCCH_3(OH)_2$ (loss of Cl^-)	314.8
$CNCCH_3(OH)_2$	343.9

$NO_2CCH_3(OH)_2$	326.0
$CH_3CH_2CH_2CCH_3(OH)_2$	363.7
$CH(CH_3)_2CCH_3(OH)_2$	363.4
$CH_3CH_2CH_2CH_2CCH_3(OH)_2$	363.3
$CH(CH_3)(CH_2CH_3)CCH_3(OH)_2$	361.8
$CH(CH_3)_2CH_2CCH_3(OH)_2$	361.3

Table 3. G3(MP2) Lewis acidities (ΔH for $AOH^- \rightarrow A + OH^-$) in kcal/mol at 298 K

Molecule	**OH^- Lewis Acidity**
$CH_2O_2H^- \rightarrow CH_2O + OH^-$	32.5
$CHCH_3O_2H^- \rightarrow CHCH_3O + OH^-$	32.3
$C(CH_3)(C_2H_5)O_2H^- \rightarrow C(CH_3)(C_2H_5)O + OH^-$	32.7
$C(C(CH_3)_3)(CH_3)O_2H^- \rightarrow C(C(CH_3)_3)(CH_3)O + OH^-$	35.5
$CH(CH_3)_2CCH_3O_2H^- \rightarrow CH(CH_3)_2CCH_3O + OH^-$	34.9
$CH_3CH_2CH_2CCH_3O_2H^- \rightarrow CH_3CH_2CH_2CCH_3O + OH^-$	33.4
$CH_3CH_2CH_2CH_2CCH_3O_2H^- \rightarrow CH_3CH_2CH_2CH_2CCH_3O + OH^-$	33.8
$CH(CH_3)(CH_2CH_3)CCH_3O_2H^- \rightarrow CH(CH_3)(CH_2CH_3)CCH_3O + OH^-$	34.2
$C(CH_3)(CF_3)O_2H^- \rightarrow C(CH_3)(CF_3)O + OH^-$	53.6
$C(C_6H_5)(CH_3)O_2H^- \rightarrow C(C_6H_5)(CH_3)O + OH^-$	37.0
$FCCH_3O_2H^- \rightarrow FCCH_3O + OH^-$	43.2
$CNCCH_3O_2H^- \rightarrow CNCCH_3O + OH^-$	54.1
$NO_2CCH_3O_2H^- \rightarrow NO_2CCH_3O + OH^-$	76.5
$ClC(CH_3)O_2H^-$ (Cl ...CH_3) $\rightarrow ClC(CH_3)O + OH^-$	72.6
$ClC(CH_3)O_2H^-$ (Cl ...HO) $\rightarrow ClC(CH_3)O + OH^-$	86.0

Bond Dissociation Energies in Second Row Compounds: The Definition of a Bond Energy

Heats of formation at 0 K and 298 K were predicted for PF_3, PF_5, PF_3O, SF_2, SF_4, SF_6, SF_2O, SF_2O_2, and SF_4O as well as a number of radicals derived from these stable compounds on the basis of CCSD(T) calculations extrapolated to the complete basis set limit. In order to achieve near chemical accuracy (± 1 kcal/mol), additional corrections were added to the complete basis set binding energies based on frozen core coupled cluster theory energies: a correction for core-valence effects, a correction for scalar relativistic effects, a correction for first order atomic spin-orbit effects and vibrational zero point energies. The calculated values substantially reduce the error limits for these species. A detailed comparison of adiabatic and diabatic bond dissociation energies (BDEs) were made and used to explain trends in the BDEs. Because the adiabatic BDEs

of polyatomic molecules represent not only the energy required for breaking a specific bond but also contain any reorganization energies of the bonds in the resulting products, these BDEs can be quite different for each step in the stepwise loss of ligands in binary compounds. For example, the adiabatic BDE for the removal of one fluorine ligand from the very stable closed shell SF_6 molecule to give the unstable SF_5 radical is 2.8 times the BDE needed for the removal of one fluorine ligand from the unstable SF_5 radical to give the stable closed shell SF_4 molecule. Similarly, the BDE for the removal of one fluorine ligand from the stable closed shell PF3O molecule to give the unstable PF_2O radical is higher than the BDE needed to remove the oxygen atom to give the stable closed shell PF_3 molecule. The same principles govern the BDEs of the phosphorous fluorides and the sulfur oxofluorides. In polyatomic molecules, care must be exercised not to equate BDEs with the bond strengths of given bonds. The results in combination with singlet-triplet splittings enable us to compare the adiabatic and diabatic BDEs. In diatomics, the BDE is a direct measure for the bond strength, and frequently the same assumption is applied incorrectly to polyatomic species for which reorganization energies in the product are important. Therefore, for polyatomic species, adiabatic bond dissociation energies and bond strengths are not the same and a clear distinction must be made between the two. The measurement of the strength or stiffness of a given bond involves only a small displacement of its atoms and no reorganization of the molecule. Appropriate criteria for judging the bond strength include the curvature of the bond energy plots, bond lengths, vibrational frequencies, force constants, bond orders, etc, and it is these that form the basis for writing representative valence bond structures for polyatomic molecules in their ground states. The differences between the adiabatic and diabatic BDEs, which are related to the reorganization energy in the products, can be estimated in the molecules under study from singlet-triplet splittings. The reorganization energies can account for the large fluctuations in adiabatic BDEs observed during the stepwise loss of fluorine atoms. In contrast, the diabatic BDEs of a given type are often very similar in size to each other and thus exhibit more regular trends. The measurement of the bond strength or stiffness of a given bond represented by its force constant involves only a small displacement of the atoms near equilibrium and, therefore, does not involve any reorganization energies, i.e., it may be more appropriate to correlate with the diabatic product states.

Additional Related Supported Studies

Microstructures Nanopore-Walled Porous Silicon as an Anode Material for Rechargeable Lithium Batteries: Porous silicon (PS) with a micro-nano-hybrid structure has been successfully fabricated with an electrochemical etching process. The micropores consist of one-dimensional tunnels, which vary from ca. 1 to 1.5 μm in pore diameter and extend up to 15 μm in depth. The walls of these micropores are covered with a nanoporous structure that consists of small spherical particles, the feature size of which is of the order of tens of nanometers or smaller. The as-prepared PS structures show cathodic/anodic peaks for lithiation/delithiation during cyclic voltammetry with minimal destruction of either the micropore or nanopore of its wall even after 50 cycles. Furthermore, the peak current, the cumulative charge increase, and the electrochemical impedance for electrode reactions consistently decreases with the surface area of the tunnel wall, indicating that processes at the tunnel wall govern the overall lithiation/delithiation reactions. A hybrid porous structure consisting of microtunnels with nanostructured surface layers appears to provide a viable and practical way to utilize silicon for anode materials in rechargeable

The Potential of Porous Silicon Gas Sensors Recent developments in porous silicon gas sensors have been reviewed. Detected species detection levels and the mechanisms of sensing for different sensor designs are also discussed. Porous silicon surface modification methods are employed for detecting different gas molecules; H_2O, ethanol, methanol, isopropanol, CO_x, NH_3, O_2, H_2, HCl, SO_2, H_2S, and PH_3.

Broader Impacts

Both the Dixon and Gole groups have significant numbers of undergraduate researchers. The Gole group has 5 undergraduates, two of which are women. The female undergraduate students at Georgia Tech have received research awards/scholarships as noted below. The Dixon group had 9 undergraduate research students, four of whom are women. The female undergraduate students at The University of Alabama have received research awards/scholarships as noted below. Both sets of undergraduate students have been involved in a number of research presentations. The undergraduate students have won a significant number of awards. The results from the research effort are being used in the Freshman Learning Community taught by Dr. Dixon at UA to introduce freshmen to research in the sciences as well as the impact of science and technology on dealing with issues in terms of energy and the environment.

The work is having an impact on the design of new sensors and new photocatalytic processes involving TiO_2 which can be used in removing organic contaminants or improving reaction selectivity.

Publications

a) Published

1. "Evidence for High Spin Transition Metal Ion Induced Infrared Spectral Enhancement," J. L. Gole, S. M. Prokes, M. G. White, T.-H. Wang, R. Craciun, and D. A. Dixon, *J. Phys. Chem. C*, **2007**, *111*, 16871.

2. "Optical and Electronic Properties of Semiconducting Nanostructures for Photocatalytic Hydrogen Generation," A. Ogden, J.L. Gole, and A.G. Fedorov, *J. Nanoelectronics and Optoelectronics I,* invited, *2*, 269-277 (2007).

3. "Development of Porous Silicon-based Active Microfilters," Jenna Campbell, James A. Corno, Nicole Larsen, and James L. Gole, *J. Electrochem*. Soc., *155*, D128-D132 (2008).

4. "Efficient Room Temperature Conversion of Anatase to Rutile TiO_2 Induced by High Spin Ion Doping," James L. Gole, Sharka M. Prokes, and Orest J. Glembocki, *J. Phys. Chem. C*, 112, 1782-1788 (2008).

5. "Diffusion Controlled Self-Assembly and Dendritic Formation in Silver Seeded Anatase Titania Nanospheres," James A. Corno, John Stout, Rusen Wang, and James L. Gole, *J. Phys. Chem. C*, *112*, 5439-5446 (2008).

6. "Bond Dissociation Energies in Second Row Compounds," D. J. Grant, M. H. Matus, J. Switzer, D. A. Dixon, J. S. Francisco, and K.O. Christe, *J. Phys Chem A.*, **2008**, *112*, 3145

7. "Experimental and Theoretical Studies of the Photoreduction of Copper(II)-Dendrimer Complexes," H. Wan, S. Li, T. A. Konovalova, S. Shuler, D. A. Dixon, and S. C. Street, *J. Phys. Chem C.*, **2008**, *112*, 1335

b) Accepted for Publication:

1. "Metal Ion Induced Room Temperature Phase Transformation and Stimulated Infrared Spectroscopy on TiO_2 – based Surfaces," James L. Gole, S.M. Prokes, and Mark G. White, *Applied Surface Science*, accepted.

2. "Multiscale Mass Transport in Porous Silicon Gas Sensors," Peter A. Kottke, Andrei G. Fedorov, and James L. Gole, in *Modern Aspects of Electrochemistry,* M. Schlesinger editor, Springer, in press.

3. "Molecular Structures and Energetic of the $(TiO_2)_n$ (n = 1−4) Clusters and Their Anions," S. Li and D. A. Dixon, *J. Phys. Chem. A*, accepted, April, 2008

c) Submitted for Publication:

1. "A Comparative Study of Simultaneous Cobalt (II) Ion Seeding of TiO_2 and $TiO_{2-x}N_x$ at the Nanoscale: Evidence for Formation of Spinel Structure and Binding Energy Modification in the Room Temperature Conversion of Anatase to Rutile TiO_2," James L. Gole, Sharka M. Prokes, Xiaofeng Qiu, Clemens Burda, and Orest J. Glemboki, *Surface Science*, submitted.

2. "Maintaining Particle Size in the Transformation of Anatase to Rutile Titania Nanostructures," Andrew Ogden, Andrei Fedorov, Jong-il Hong, and James L. Gole, *Chem. and Phys. Solids*, submitted.

3. "The Surprising Average Oxidation State of Fumed Silica and the Nature of Water Binding to the Silicon Oxides and Hydroxides," James L. Gole, Mark G. White, Tsang-Hsiu Wang, and D.A. Dixon, *Chemical Communications*, submitted.

4. "Active Microfiltered Sensor Interfaces, Photocatalytic Reactors, and Microbatteries Using Combined Micro/nanoporous Interfaces," James L. Gole, James Corno, Serdar Ozdemir, Sharka Prokes, and Heon-Cheol Shin, Phys. Stat. Solid, submitted.

5. "The Potential of Porous Silicon Gas Sensors," Serdar Ozdemir and James L. Gole, invited in *Current Opinions in Solid State and Materials Science*, submitted.

d) Planned (partially completed) Publications:

1. "Water to Hydrogen Conversion from Water Ligated Transition Metal Ion Complexes Trapped on Titania or Titanium Oxynitride Nonocolloids," James L. Gole, Andrei Fedorov, Sharka Prokes, Clemens Burda, and David A. Dixon, *J. Phys. Chem.*, to be submitted.

2. "Nitrogen Fixation in Metal Ion Seeded $TiO_{2-x}N_x$ Nanoparticles," James L. Gole, Mark G. White, Xiaofeng, Qiu, Clemens Burda, and H.J. Martin.

3. "Activity of Shifting Nanoscale Silicon Oxide Oxidation State Distributions: The Transformation from Hydrophilicity to Hydrophobicity," James L. Gole, Mark G. White, William Laminack, Serdar Ozdemir, A.G. Ogden, and H.J. Martin.

Presentations

1. Ogden, A., Gole, J. L., and Fedorov, A., Synthesis and characterization of $TiO_{2-x}N_x$ nanostructures for visible light photocatalytic hydrogen production, *2nd ASME Energy Nano Conference*, Santa Clara, California, September 5-7, 2007.

2. Ogden, A., Gole, J. L., and Fedorov, A., Synthesis and characterization of $TiO_{2-x}N_x$ nanostructures for visible light photocatalytic hydrogen production, *Renewable and Sustainable Technologies Research Poster Competition*, Georgia Institute of Technology, Atlanta, Georgia, April 16, 2008.

3. Gole, James L. ICFSI "11th International Conference on the Formation of Semiconductor Interfaces, From Semiconductors to Nanoscience, and Applications with Biology, August 19-24, 2007, "Nanostructures and Porous Silicon: Activity at Interfaces in Sensors and Photocatalytic Reactors."

4. Gole, James L. Perimeter Adult Learning Center (PALS), October 15, 2007, "An Introduction to the Ideas of Nanotechnology", October 22, 2007, "Sensors, Microreactors, and Microfiltration – From Nanostructures to Porous Silicon."

5. Gole, James L. University of Alabama, Departments of Chemistry and Physics, November 19, 2007, "Nanostructures and Porous Silicon: Activity at Interfaces in Sensors and Photocatalytic Reactors."

6. Gole, James L. Naval Research Laboratory, March 2008, Nanostructures and Porous Silicon: Activity at Interfaces in Sensors and Photocatalytic Reactors.

7. J. Gole, PSST: March 2008, "Active Microfiltered Sensor Interfaces, Photocatalytic Reactors, and Microbatteries."

8. Gole, James L. Mississippi State University, Department of Chem Eng. And Physics, April 15, 2008, "Nanostructures and Porous Silicon: Activity at Interfaces in Sensors and Photocatalytic Reactors."

9. Gole, James L. University of Southern Mississippi, Department of Physics, April 16, 2008, "Nanostructures and Porous Silicon: Activity at Interfaces in Sensors and Photocatalytic Reactors."

10. Jamie Hennigan, T.-H. Wang, S. Li, J.L. Gole, and David A. Dixon, 7th Annual University of Alabama System Honors Research Conference, "Computational Density Functional Theory Studies of the Binding Energies of Group IVB Transition Metal Oxide Nanoclusters," Poster, April 11, 2008, University of Alabama at Birmingham, Birmingham AL. (undergrad)

11. Emily Wayman, T.-H. Wang, S. Li, and David A. Dixon, 7th Annual University of Alabama System Honors Research Conference, "Computational Studies of Titanium Nanoclusters," Poster, April 11, 2008, University of Alabama at Birmingham, Birmingham AL. (undergrad)

12. Jackson Switzer, Myrna H. Matus, Daniel Grant, and David A. Dixon, 7th Annual University of Alabama System Honors Research Conference, "Energetics Relevant to the Atmospheric Decomposition of Chemical Weapons," April 11, 2008, Poster, University of Alabama at Birmingham, Birmingham AL. (undergrad)

13. Jamie Hennigan, T.-H. Wang, S. Li, J.L. Gole, and David A. Dixon, The University of Alabama System Undergraduate Research Conference, "Computational Density Functional Theory Studies of the Binding Energies of Group IVB Transition Metal Oxide Nanoclusters," Poster, April 21, 2008, The University of Alabama. (undergrad)

14. Emily Wayman, T.-H. Wang, S. Li, and David A. Dixon, The University of Alabama Undergraduate Research Conference, "Computational Studies of Titanium Nanoclusters," Poster, April 21, 2008, The University of Alabama. (undergrad)

15. Jackson Switzer, Myrna H. Matus, Daniel Grant, and David A. Dixon, The University of Alabama System Undergraduate Research Conference, "Energetics Relevant to the Atmospheric Decomposition of Chemical Weapons," Poster, April 21, 2008, The University of Alabama. (undergrad)

16. Tsang-Hsiu Wang, Raluca Craciun, David A. Dixon, and James L. Gole, "Induced infrared spectral enhancement in doped TiO_2," Poster, American Chemical Society National Meeting, New Orleans, April 5 -10, 2008, The University of Alabama. (grad student)

17. Tsang-Hsiu Wang, Raluca Craciun, David A. Dixon, and James L. Gole, "Induced infrared spectral enhancement in doped TiO_2," Poster, SETCA 2008, May 16 and 17, 2008, The University of Alabama. (grad student)

18. David A. Dixon, "Computational Advances in Predicting the Behavior of Inorganic Compounds," Department of Chemistry, University of South Alabama, Mobile AL Feb. 2008.

19. David A. Dixon "Computational Advances in Predicting the Behavior of Inorganic Compounds," Feb. 8, 2008, Department of Chemistry, University of North Texas, Denton TX

Awards and Recognition

(1) Jenna Campbell (GaTech undergrad) was the recipient of the Best Undergraduate Research Award from the Georgia Tech Chapter of Sigma Xi.

(2) Nicole Larsen (GaTech undergrad) was the recipient of a 2007 Astronaut Fellowship and the Hitohiro Fukuyo Memorial Scholarship from Georgia Tech School of Physics.

(3) William Laminack (GaTech undergrad) was the recipient of the Outstanding Physics Undergraduate Award.

(4) James L. Gole was the recipient of the Georgia Tech Outstanding Undergraduate Research Mentor Award.

(5) Andrew Ogden (GaTech graduate student working on the project) received the 3rd place award at the Renewable and Sustainable Technologies Research Poster Competition by the Brook Byers Institute for Sustainable Systems, Georgia Institute of Technology.

(6) Jenna Campbell (GaTech undergrad) was the recipient of a 2008 Astronaut Fellowship.

(7) Emily Waymans was chosen as Outstanding Freshman of the Year at The University of Alabama.

(8) Jackson Switzer (UA undergrad) was a 2008 USA Today 2nd Team All Academic Team member.

(9) Jackson Switzer (UA undergrad) received a Dean's Award of Merit.

(10). Dr. Szulczewski will receive funding from the Irish Science Foundation (E.T. S. Walton Visitor Award) to support his sabbatical stay at Trinity College in Dublin from September 2008 until the summer of 2009.

NIRT: Active Nanoparticles in Nanostructured Materials Enabling Advances in Renewable Energy and Environmental Remediation

Final Report, September, 2011

Overview

Our research efforts during this period have involved a combined experimental and computational characterization of the behavior of active nanostructures. We have been concerned with the formation and study of unique porous silicon interfaces and the characterization of uniquely doped and modified TiO_2 nanostructures. We have developed a new approach to the design of sensors and catalysts on such surfaces based on the inverse hard and soft acid base (IHSAB) model.

Porous Interfaces and the IHSAB Model. Much of our experimental focus on the extension year was the continued development and validation of the IHSAB model and its use in the development of new sensor technologies. A key emphasis in our experimental effort has been the introduction of active nanostructures to active interfaces. We have demonstrated a framework for such studies. Nanopore covered micro-porous silicon (PS) interfaces can be transformed to create highly active reversible sensor configurations for the detection of gaseous or aqueous analytes. Within this framework, we have discovered that nanostructured oxides introduced to the PS interface can provide a means to control the physisorption/ chemisorption processes on an extrinsic semiconductor surface and can be used to create an array of sensor responses for a variety of gases. We are continuing our development of a general model for these highly active, treated interfaces, which takes advantage of the playoff between the chemical bonding and physical adsorption associated with the deposited nanostructured oxides. A means to improve the reversible, sensitive, and selective response to basic (Lewis definition = available electrons) analytes results in an increase in the resistance characteristic of the response of p-type silicon (resistance decreases for an n-type semiconductor or for the interaction of an electron acceptor). The gaseous base contributes an electron to the PS surface which diminishes the majority carriers. The approach, counter to one which promotes significant chemical bond formation via HSAB interactions, promotes the enhancement of physisorption. Our newly developed IHSAB model for the interaction of gases is to minimize chemical bonding to maximize electron transfer to the PS-based interface. Our IHSAB model is based on the HSAB concept developed by Pearso and later correlated within the context of Density Functional Theory (DFT) by Pearson, Parr, and others. The IHSAB model is somewhat broader-based, predicts reversible sensor-analyte interactions and, in conjunction with extrinsic semi-conductors, predicts observable resistance changes. An array of responses is created as the nanostructure deposits are chosen to provide a range of sensitivities for a given analyte based largely on the physisorption which the nanostructured deposit can enhance for that analyte. The concept, based on the reversible interaction of hard acids and bases with soft bases and acids enables the selection of sensor and analyte materials which do not interact to form strong covalent or ionic chemical bonds. The IHSAB concept, implemented on “phase matched” nanoporous silicon layers (Figure 1), has been demonstrated to provide significant and predictable changes in sensor sensitivity for a variety of analytes. The concept introduces selectivity within a matrix of variable responses for a given analyte. It is important to note that the nanostructured deposits act as antennas to focus the

nature of the chemical interaction with the semiconductor majority charge carriers. This provides a strong control of the balance of separation between physical and chemical interactions. The development of efficient microreactors can also rely on this balance. In concert with the metal ion seeding and deposition of photocatalytic nanostructures, we form a framework for the design of solar pumped sensors.

The selective fractional deposition of nanostructured materials can be used to create inexpensive microfabricated sensor arrays with integrated CMOS circuits, and we are developing "materials selection tables" built on our IHSAB model. Materials including Au_xO, SnO_2, Cu_xO, NiO, nanoaluminum, and nanotitania have already been demonstrated for the detection of gases including NH_3, PH_3, CO, H_2S, and SO_2 in an array-based format at the sub-ppm level. The results we have obtained for PH_3, NH_3, and NO are summarized in Table 1. In complement, the configuration of Figure 1 is also ideally suited for use in microreactor design.

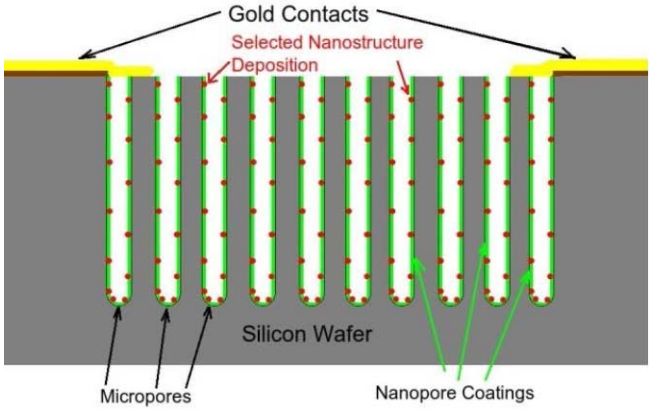

Figure 1 Schematic diagram of hybrid etched nanopore covered microporous porous silicon (PS) array coated with selected nanostruc-tures. Au contacts are deposited onto the PS via a SiC insulation layer on the c-Si surface.

Table 1. ΔR(coating)/ΔR(uncoated) values for impedance changes at 1 ppm as compared to an uncoated PS sensor.

Molecule	SnO_2	NiO	Cu_xO	Au_xO
PH_3	2	2.5	4	5
NO	7-10	3.5	1	1.5
NH_3	1.5	1.5-2	2-2.5	~3

The combination of nanopore covered micropores shown in Figure 1 provides for enhanced diffusion of the analyte gas to active sites[7]. The micropores provide for Fickian diffusion whereas the rate limiting diffusion of analyte gas results from Knudsen diffusion through the nanopore wall coating of the micropores (Figure 1). Deposition of this hybrid surface with metal oxide nanoparticles/clusters introduces new selective sites and an enhanced response relative to the untreated PS interfaces as exemplified in Table 1. This enhanced response is manifest by a resistance increase when gaseous bases interact with an acidic nanostructure treated "p-type" PS interface. The increased resistance results as electrons transferred from the basic analyte to the modified "p-type" surface decrease the majority carriers. The ratio of responses is directly related to the variation of surface acidity, from hard to soft, introduced by the nanostructures. This configuration can be used at the nanoscale to distinct advantage not only in sensor but also micro-reactor design, here, again, using variants of the HSAB principle.

The facile oxidation state changes for the transition metal halides which we have observed are significant for the design of photoelectrochemical cells. Because of this behavior, we are extending our framework for the seeding and doping of TiO_2 and its oxynitride, in part, because of the unexpected phase transformations and modifications which have been observed in these systems. We continue to focus on the ready electron removal to TiO_2 and its oxynitride, when

these nanostructures are seeded with the transition metal halides. We suggest that electrodes prepared with transition metal halide seeded TiO_2 ($TiO_{2-x}N_x$) may offer viable and improved alternatives to solid state photovoltaic as well as Grätzel-type cells. We have performed promising cyclic voltammetry experiments in which the working electrodes correspond to Co^{+2}, Fe^{+2}, Fe^{+3}, and Mn^{+2} chloride seeded $TiO_{2-x}N_x$ ($KCl(K_2SO_4)$/water(methanol) electrolyte). These experiments are designed to make use of visible light induced redox couples based upon the observed changes in the XPS spectra of nitrogen doped and transition metal ion seeded TiO_2. Initial experiments indicate a substantial reduction $Ti^{4+} \rightarrow Ti^{3+}$, the rate of which is strongly influenced by Fe^{+2} seeding. The process is also affected (shift in cyclic voltammogram) by the introduction of visible incandescent light. This suggests the possibility of using visible light induced changes in the oxidation state of Co, Fe, or Mn to transfer electrons to a TiO_2 based framework which, especially in the case of the oxynitride, can be effectively connected to an external electrode. The presence of the Cl^- counterions from the metal halide can furnish an effective hole sink as they form Cl atoms. These Cl atoms, with their substantial electron affinity can recapture electrons from the solvent solution completing an electrochemical cycle. Thus we have an alternative to the traditional Grätzel cell (an MHSC cell) and a potential material for solid state photovoltaic MHPV cells.

New Electrode Development for Photocatalytic Applications. The 3^+ eV bandgap of TiO_2 based photocatalysts limits its utility for solar energy harvesting due to an energy mismatch with the solar spectrum. To improve solar energy utilization, band gap reduction using cationic and anionic doping techniques has been demonstrated by others. To maximize charge carrier lifetimes, it has been shown in the literature that the intrinsically weak electrical conductivity of TiO_2 nanoparticulate layers requires that the semiconductor layer thickness be less than ~1 micron. However, we have demonstrated that as the layer thickness is reduced, the stability of the layer in operation can be severely compromised (unpublished work, Gole and Federov). During photocatalytic hydrogen production, the water splitting reaction on TiO_2 generates oxygen gas within the nanoporous electrodes. We have hypothesized that this internal oxygen evolution produces significant internal pressurization of the porous layer. Three principal layer failure modes have been described in the literature - pitting failure of the TiO_2 particulate layer, chemical attack of the substrate, and delamination of the layer from the substrate. All three failure mechanisms for nanoparticulate TiO_2 layers are enhanced as the layer thickness is reduced.

As coating technologies such as spin and dip-coating have not been shown to generate thin and robust TiO_2 nanoparticle layers, we have investigated the generation of a new type of interfacial contact. It is expected that the formation of a metal-TiO_2 hybrid interface through local melting will achieve enhanced mechanical strength and electrical conductivity at the substrate-TiO_2 layer interface. However, we have also demonstrated that the rapid thermal treatment in excess of 600^oC with nitrogen doped anatase TiO_2 causes phase transformation into the less desirable rutile phase. In order to maintain both large dopant content, as well as the desirable anatase phase, both high temperatures and rapid heating must be avoided during electrode preparation. As the melting temperature of conductive substrate materials such as aluminum is in excess of 650^oC, the deposition of highly doped anatase TiO_2 onto such a molten material would lead to undesirable phase transformation.

In order to generate the desired interfacial contact of doped anatase TiO_2 and a conductive substrate, a new contact preparation methodology has been developed. Prior experimental and theoretical work by others shows that when a material length scale of a metal particle or asperity is on the order of a few nanometers, the large local curvature increases the surface free energy which reduces the melting temperature. Thus the generation of a surface with a regular arrangement of nanometric features would allow for local melting of the metal surface at much lower temperatures that those required for bulk melting. Once molten, the impregnation of TiO_2

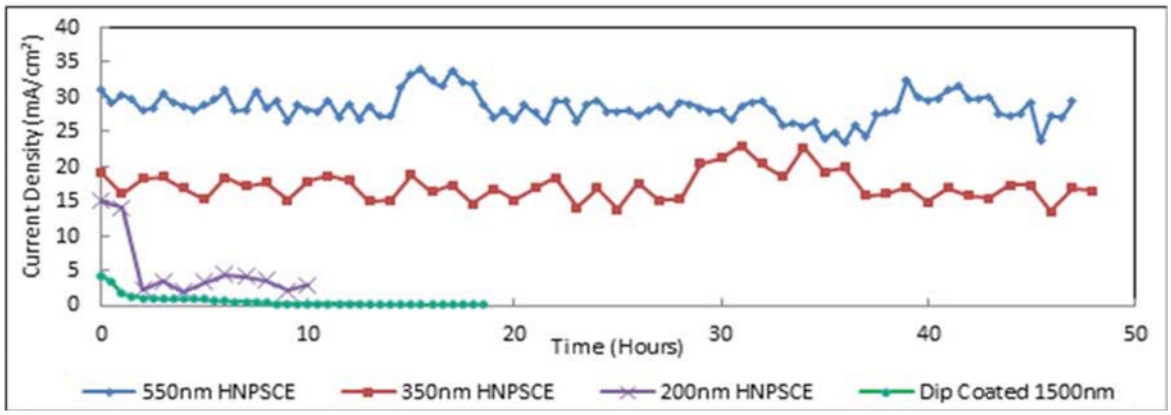

Figure 1 Photoelectrochemical Performance of TiO_2 Nanoparticle Based HNPSCE vs. Dip Coated Electrodes

nanoparticles directly into the metal should be achievable avoid undesirable anatase-to-rutile transformation characteristic of high temperature processing. To implement this design, we utilize porous anodic alumina fabrication techniques in which a pure aluminum sheet is oxidized at 0^oC in 3 Molar oxalic acid solution at 40V applied potential versus a graphite counter electrode. The resultant aluminum oxide surface is restructured with 100nm pits in a honeycomb pattern. Subsequent oxide stripping in a chromic and phosphoric acid solution at 70^oC results in an oxide free aluminum surface with the same honeycomb pattern of pitting. At the interface between two pits lies a high aspect ratio aluminum projection with reduced melting temperature. We have utilized AFM and SEM to demonstrate that this layer undergoes significant structural reformation and softening upon heating to temperatures below the melting point of bulk aluminum. To utilize this nanostructure-facilitated local melting and generate interfacial contact of aluminum and TiO_2, a solution of TiO_2 nanoparticles suspended in methanol is sprayed onto the nanostructured aluminum surface while it is heated from underneath to $350\text{-}550^oC$. The flash evaporation of the methanol solvent provides a phase change cooling buffer layer to prevent thermally shocking the TiO_2 particles, thus avoiding undesirable solid phase transformation. The resultant electrode structure is termed the hybrid nanopatterned and spray-coated electrode (HNPSCE).

Photoelectrochemical hydrogen production with the resultant hybrid interfaced photoelectrodes has shown up to a 1200% increase in the hydrogen production rate compared to a dip coated sample of the same nanoparticles. Even more significant is that these hybrid electrodes demonstrate stable hydrogen production rates for greater than 40 hours without evidence of structural failure. The performance improvement and long term stability of the HNPSCE electrodes is shown in Figure 1. The hydrogen production rate is shown by proxy through the

cell electrical current, where higher currents indicate a greater hydrogen production rate. It is evident that the thicker sample, labeled 550nm HNPSCE, outperforms all other samples of the HNPSCE. The thicker TiO_2-coating HNPSCE electrodes (550nm and 350nm in Figure 1) exhibit the long term stability, whereas, the thinner coating sample labeled 200nm HNPSCE shows performance degradation after 2 hours of operation. All HNPSCE electrodes however demonstrate improved performance over the thicker dip-coated sample, which experienced rapid layer dissolution and performance degradation after 30 minutes of operation.

Electrode Structural Characteristics

Contacting Layer: The HNPSCE electrode is composed of three distinctly structured layers of TiO_2 particles described here as the contacting, compact, and aggregate layers. The contacting layer is made up of TiO_2 nanoparticles embedded into the nanostructured aluminum substrate. It is notable that the contacting layer is composed of very few contact points between the photocatalyst nanoparticles and the metal substrate, with the distance between embedded particles of ~3-10 greater than the particle diameter, typically 300-1000 nm. The embedded TiO_2 nanoparticles serve as anchor points between the aluminum substrate and the compact TiO_2 layer. The irregular contact pattern of this layer is shown in the FIB/TEM image of Figure 2(a),

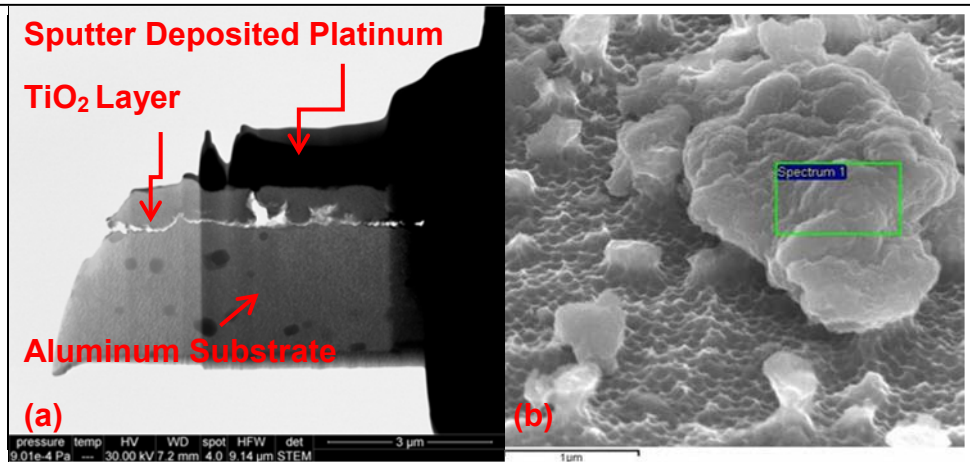

Figure 2: (a) FIB sectioned SEM Image of HNPSCE Electrode Contacting and Compact Layer Structure and (b) 45° Tilt SEM Image of Contacting layer morphology generated from short duration spray of TiO_2-methanol solution

where the TiO_2 layer has been capped with a platinum overlayer for FIB cutting. The contacting behavior is complex and demonstrates a constricted contact area with respect to the total surface area of the aluminum substrate. Another image of the contacting layer structure is shown in Figure 2(b) where a short duration spray of the TiO_2-methanol solution was used to obtain a clear view of the interface without forming the outer compact and agglomerated layers. The nanopatterned aluminum substrate is clearly visible, with the white agglomerated particles adhered to the surface being TiO_2 as verified by EDX and XPS spectroscopic techniques. We are currently investigating the influence of contact area and possible aluminum-TiO_2 alloying on interfacial electrical contact resistance using conductive force microscopy (CFM).

Compact Layer The second distinct layer of the HNPSCE structure is composed of sintered TiO_2 nanoparticles which exhibit minimal porosity. Shown in Figure 3 is a top down SEM image

of the compact layer after repeated rinsing in ethanol has removed the outer agglomerated layer. It is notable that a fully densified and continuous compact layer is not achieved until a coating thickness of approximately 330nm is produced. It has been demonstrated that a continuous compact layer is needed to prevent the electrolyte from permeating the HNPSCE electrode and degrading the aluminum substrate. The 200nm HNPSCE electrode of Figure 1 for example did not have a continuous compact layer and exhibited pitting failure of the aluminum substrate within 2 hours of operation. The average pore radius of this sintered structure is ~3-5nm from the BET nitrogen adsorption technique. Instrumented Nanoindentation (INI) testing was performed to investigate the mechanical strength and hardness of this layer. A view of the in-layer structure is shown in Figure 3(bottom), where repeated thermal cycling coupled with the mismatch of thermal expansion coefficients of aluminum (22.2E-6 K^{-1}) and TiO_2 (9E-6 K^{-1}) has ruptured the compact layer. Also demonstrated in this image is the 'floating island' behavior of the compact layer, held in place only by the 'anchor points' of the contacting layer.

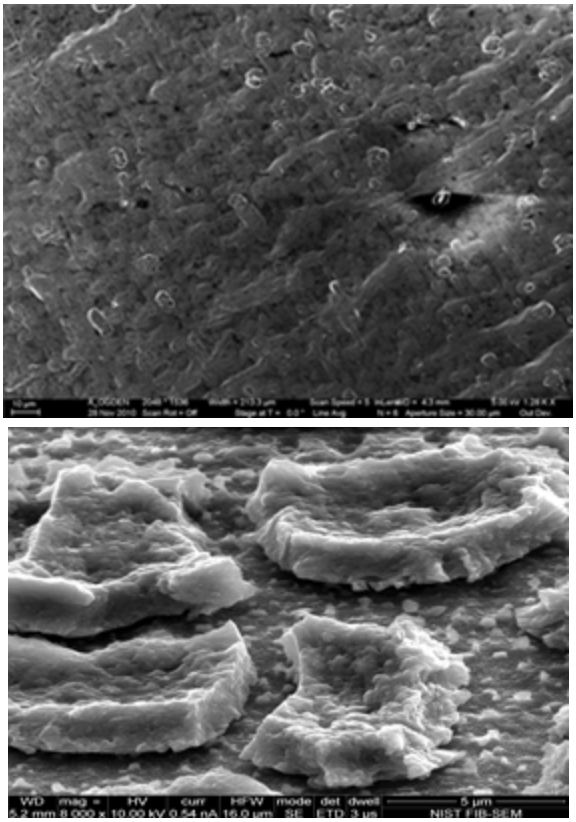

Figure 3: (Top) SEM Image of HNPSCE Compact layer and (Bottom) Edge view of ruptured Compact Layer generated through repeated thermal cycling

Agglomerated Layer Furthest from the aluminum substrate is a weakly adhered layer of agglomerated TiO_2 nanoparticles of much higher porosity than the compact layer, with an average pore radius of 11-46 nm from BET. The surface of the agglomerated layer is irregular with dendrite-like projections. The irregular surface morphology is displayed in SEM image of Figure 4(Top). As the aggregate layer is only weakly sintered during spraying, it exhibits a resistance to deformation under indentation which is several orders of magnitude less than that of the compact layer. As prepared the layer is adhered so weakly to the surface that it is rapidly removed during the initial 30 seconds of operation during photocatalytic hydrogen production. However, once the material is annealed at temperatures exceeding 350^{o}C for 15 minutes or more, the particles begin to sinter together and form much more rigid structures as shown in the SEM image of Figure 4(Bottom). It is critical to note that the photocatalytic performance of the HNPSCE electrode is highly dependent on the agglomerate layer. Sintered electrodes produce hydrogen at rates 200-600% above that of non-sintered electrodes.

We believe that the performance advantage of the sintered electrodes is composed of three principal interactions - surface area enhancement, an increase in an apparent light absorbance, and ionic species transport enhancement, all of which are dependent on the structure of the agglomerate layer. The kinetics of the oxygen generation reaction on TiO_2 surfaces are reported

to be very slow, and thus increases in catalytically active surface area will play a key role in improving hydrogen production rates. In addition, the linear absorption coefficient of TiO_2 is only ~$6.6x10^{-3}$ cm^{-1} at the absorption edge. Because of this weak absorption coefficient, a thin planar layer of TiO_2 such as the compact layer alone is not sufficient to absorb all incident solar photons. Thus the addition of the complex structures of the sintered agglomerate layer may play a key role in boosting operational yield by enhancing effective light absorption through multiple reflections. The interplay between these effects and their contributions to the significant performance enhancement from the sintered agglomerate layer are still under investigation utilizing cyclic voltammetry, optical reflection studies, and ionic diffusional transport modeling.

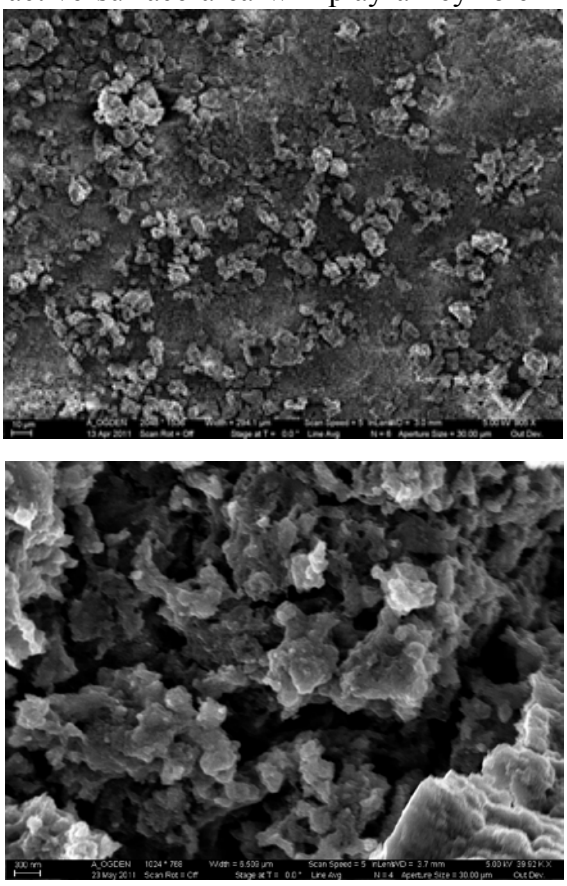

Figure 4: SEM Image of HNPSCE Electrode Aggregate Layer: (Top) As Prepared and (Bottom) Following Sintering

Room temperature synthesis of nitrogen-doped anatase TiO_2 nanocubes with fluoride-terminated surfaces The quest to synthesize nanoscale photocatalysts that display high activity with visible light to decompose organic pollutants and catalyze water splitting is very important to future environmental and energy technologies. In particular, doped TiO_2 has been studied more than any other material owing to its chemical stability, non-toxicity and abundance. However, pure TiO_2 is only photoactive active with ultraviolet radiation since its optical gap is slightly greater than 3 eV. Since the seminal work of Asahi et al. there has been intense effort devoted over the past decade to dope TiO_2 so that it absorbs radiation greater than 400 nm. The two most common methods of doping involve non- metallic anions or transition metal cations. However, there is great variability in the efficiency of such photocatalysts because these techniques produce amorphous or nanocrystalline materials, which require high temperature annealing to remove the defects. Often when the dopant is a non-metal, such as nitrogen, the impurity atoms are released from the solid-state structure upon annealing. Furthermore the annealing process is also accompanied by sintering, which results in low surface area material. We have developed a synthetic strategy that allows for incorporation of the dopant into an amorphous TiO_2 structure, followed by a second step that forms anatase nanocubes with adsorbed fluorine at room temperature. This two-step procedure allows for independent control of the dopant concentration, surface chemistry, and morphology at room temperature. Nitrogen-doped TiO_2 nanoparticles have been synthesized using sol-gel methods and subsequently transformed into the anatase phase at room temperature by aging in acidic solutions of NaF. The materials have been characterized by x-ray photoelectron spectroscopy, x-ray diffraction, diffuse reflectance spectroscopy, and scanning electron microscopy before and after the phase transformation. At low pH the fluoride ion exists mainly as HF, which promotes the dissolution

of the as-synthesized N-TiO_2. Upon aging (12-24 hours) at room temperature in low pH solutions of NaF, crystalline anatase TiO_2 nanocubes form with adsorbed surface fluoride. Most importantly, the nitrogen dopants are retained during this dissolution/deposition process. The ability to form the nitrogen-doped anatase TiO_2 nanocubes with surface adsorbed fluoride without annealing is an important step toward the preparation of visible light active photocatalysts.

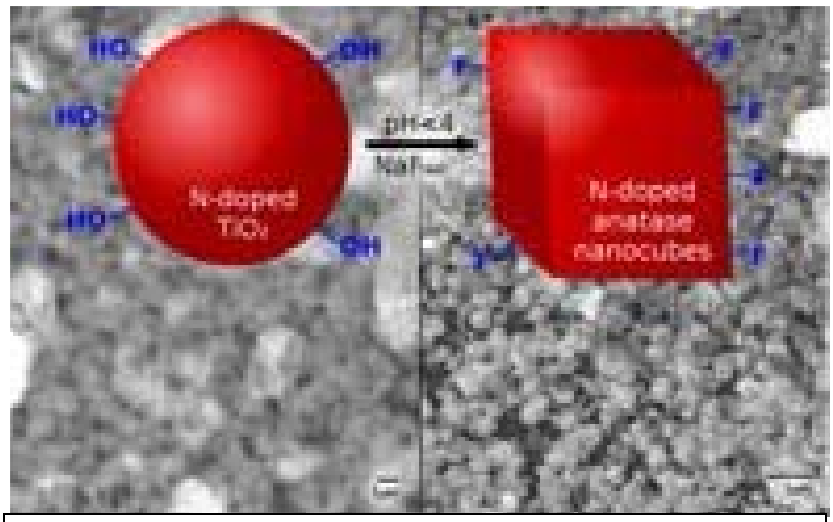

Figure 5. The SEM image on the left shows the amorphous nitrogen-doped TiO2 nanoparticles resulting from a sol-gel reaction. The SEM image on the right shows the formation of anatase nitrogen-doped TiO2 nanocubes after room temperature treatment in a pH = 2.5 solution of NaF for 24 hours.

Iron Doped metal oxide (MO_x) Interfaces of Titania and Silica. We have investigated: a) how does iron doping effect the electronic structure of the host metal centers? And (b) what oxidation states will iron be in when $FeCl_3$ is used for doping? Mixed valence states were expected based on the relative redox potentials of host and dopant. Based on the assumption of mixed valence states in the doped metal oxide, one can reasonably suspect increased catalytic activity on the Fe-doped MO_x surface. The question then arises whether varying concentrations play a greater role. Since doping at low concentrations has been studied before, we focused on the heavy-doping regime, at > 10% "dopant". The term "doping", while not precise, is used here for simplicity. Figure 6 shows an overview XPS spectrum of silica after doping with 25, 33, and 50% iron doping. Table 1 summarizes the surface composition analysis via XPS and peak deconvolution using Gaussian fitting functions.

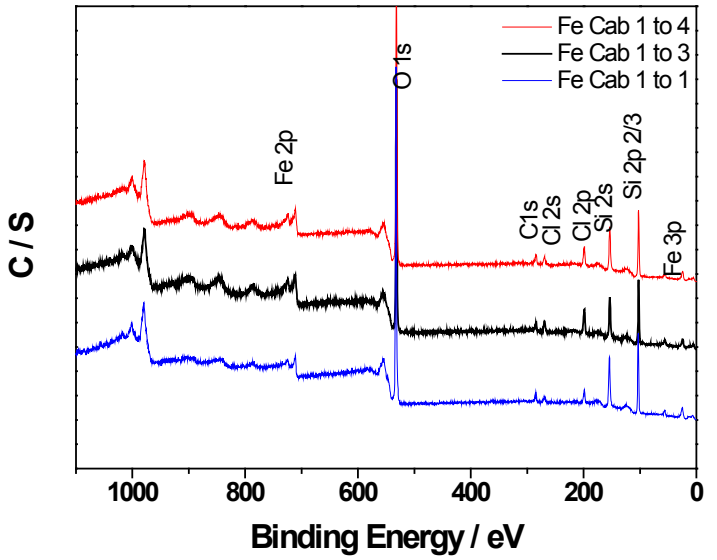

Figure 6. XPS spectra of Fe-silica samples with varying Fe/SiO_2 ratios.

Core level electrons ejected by X-rays exhibit a variety of shapes in the XPS spectra. These shapes correspond to a combination of the physics involved in the ionization process as well as

the distortions caused by the measurement mechanism. Ideally, these influences can be reflected by a mix of Gaussian-Lorentzian function, where Lorentzian describes the lifetime broadening (natural broadening) whereas Gaussian models the measurement process (instrumental response, X-ray line shape, Doppler and thermal broadening). Additionally, the XPS spectra may exhibit asymmetry due to the quantized molecular vibrational states that can be excited when a core electron is ejected by a photon. We have carefully analyzed these different aspects for XPS analysis and will publish an analytical work on this topic.

Table 1. XPS deconvoluted peaks for Fe-silica using Gaussian fitting functions

Sample	Temp. Assignment	Area/%	BE / eV	Peak width / eV	Peak height / a.u.	R^2
Fe Cab 1 to 1	($\underline{Fe}Cl_3$)*	49.4	57.1	2.9	116.9	0.996
	Fe^{3+}	46.7	55.8	1.7	189.6	
	Fe^{2+}	3.9	54.1	0.8	35.6	
Fe Cab 1 to 3	($\underline{Fe}Cl_3$)	36.1	57.6	3.6	75.5	0.995
	Fe^{3+}	54.8	55.7	2.2	183.6	
	Fe^{2+}	9.1	54.4	1.4	47.1	
Fe Cab 1 to 4	($\underline{Fe}Cl_3$)	20.2	58.3	2.8	40.5	0.997
	Fe^{3+}	65.3	55.9	2.3	159.3	
	Fe^{2+}	14.4	54.4	1.5	56.1	

Computational Studies

F^+ and F^- Affinities of Simple N_xF_y and O_xF_y Compounds Compounds with fluorine atoms adjacent to other atoms with lone pairs pose problems for computational chemistry. However, one can make reliable estimates of many of their thermomdynamic properties by the judicious use of various approaches. We are especially interested in the F^+ and F^- affinities of a broad range of compounds in order to make reactivity predictions. Given the limited experimental data available for the fluorides of nitrogen and oxygen, we have performed high accuracy theoretical calculations to determine thermodynamic properties of these molecules, namely their heats of formation and F^+ and F^- affinities. Atomization energies at 0 K and heats of formation at 0 K and 298 K are predicted for the neutral and ionic N_xF_y and O_xF_y systems using the CCSD(T) method with correlation consistent basis sets extrapolated to the complete basis set (CBS) limit. In order to achieve near chemical accuracy (± 1 kcal/mol), three corrections to the electronic energy were added to the frozen core CCSD(T)/CBS binding energies: corrections for core-valence, scalar relativistic, and first order atomic spin-orbit effects. Vibrational zero point energies were computed at the CCSD(T) level of theory where possible. The calculated heats of formation are in good agreement with the available experimental values, except for FOOF due to the neglect of higher order correlation corrections. The F^+ affinity in the N_xF_y series increases from N_2 to N_2F_4 by 63 kcal/mol, while that in the O_2F_y series decreases by 18 kcal/mol from O_2 to O_2F_2. Neither N_2 nor N_2F_4 is predicted to bind F^-, and N_2F_2 is a very weak Lewis acid with an F^- affinity of about 10 kcal/mol for either the *cis* or *trans* isomer. The low F^- affinities of the nitrogen fluorides explain why, in spite of the fact that many stable nitrogen fluoride cations are known, no nitrogen fluoride anions have been isolated so far. For example, the F^- affinity of NF is predicted to be only 12.5 kcal/mol which explains the numerous experimental failures to prepare NF_2^- salts from the well known strong acid HNF_2. The F^- affinity of O_2 is predicted to have a small positive

value and increases for O_2F_2 by 23 kcal/mol, indicating that the $O_2F_3^-$ anion might be marginally stable at subambient temperatures. The calculated adiabatic ionization potentials and electron affinities are in good agreement with experiment considering that many of the experimental values are for vertical processes. The gas phase acidity ($HNF_2 \rightarrow NF_2^- + H^+$) is 361.1 kcal/mol. There have been many unsuccessful attempts to isolate the corresponding NF_2^- anion. A likely explanation for these failures is the ease with which NF_2^- can lose an F^- anion to form NF, which can then readily dimerize in a highly exothermic reaction (92.8 kcal/mol at the CCSD(T)/CBS level plus additional corrections) to form N_2F_2 with the formation of an N=N double bond. We predict the enthalpy of the reaction $NF_2^- \rightarrow NF + F^-$ (-FA(NF), Table 6) to be only 12.5 kcal/mol at 0 K, showing that NF_2^- is only marginally stable toward F^- loss. The possibility of NF_2^- dissociating to $NF^- + F$ radicals is much less likely because this pathway is highly endothermic by 85.5 kcal/mol.

Dinitrogen Difluoride Chemistry. N_2F^+ salts are important precursors in the synthesis of N_5^+ compounds, and better methods are reported for their larger scale production. A new, marginally stable N_2F^+ salt, $N_2F^+Sn_2F_9^-$, was prepared and characterized. An ordered crystal structure was obtained for $N_2F^+Sb_2F_{11}^-$, resulting in the first observation of individual N≡N and N-F bond distances for N_2F^+ in the solid phase. The observed N≡N and N-F bond distances of 1.089(9) and 1.257(8) Å, respectively, are among the shortest experimentally observed N-N and N-F bonds. High-level electronic structure calculations at the CCSD(T) level with correlation-consistent basis sets extrapolated to the complete basis limit show that *cis*-N_2F_2 is more stable than *trans*-N_2F_2 by 1.4 kcal/mol at 298 K. The calculations also demonstrate that the lowest uncatalyzed pathway for the *trans-cis* isomerization of N_2F_2 has a barrier of 60 kcal/mol and involves rotation about the N=N double bond. This barrier is substantially higher than the energy required for the dissociation of N_2F_2 to N_2 and 2 F. Therefore, some of the N_2F_2 dissociates before undergoing an uncatalyzed isomerization, with some of the dissociation products probably catalyzing the isomerization. Furthermore, it is shown that the *trans-cis* isomerization of N_2F_2 is catalyzed by strong Lewis acids, involves a planar transition state of symmetry C_s, and yields a 9:1 equilibrium mixture of *cis*-N_2F_2 and *trans*-N_2F_2. Explanations are given for the increased reactivity of *cis*-N_2F_2 with Lewis acids and the exclusive formation of *cis*-N_2F_2 in the reaction of N_2F^+ with F^-. The geometry and vibrational frequencies of the $F_2N{=}N$ isomer have also been calculated and imply strong contributions from ionic N_2F^+ F^- resonance structures, similar to those in F_3NO and FNO. This work was highlighted with a cover on *Inorganic Chemistry*.

Selenium(IV) Fluoride and Oxofluoride Anions The three Se(+IV) fluoride and oxofluoride anions, SeF_5^-, $SeOF_3^-$ and SeO_2F^-, have been studied using experimental and theoretical methods. The $[((C_6H_5)_3P)_2N]^+$, $[(C_6H_5)_4P]^+$ and $[N(CH_3)_4]^+$ salts of SeF_5^-, SeF_6^{2-} and SeO_3F^- and $CsSeO_2F$ were prepared and characterized. Crystal structures were obtained for $[((C_6H_5)_3P)_2N][SeF_5]$ and $[((C_6H_5)_3P)_2N][SeOF_3] \cdot CH_2Cl_2$. In contrast to oxygen-bridged dimeric $TeOF_3^-$, the $SeOF_3^-$ anion in $[((C_6H_5)_3P)_2N][SeOF_3]\cdot CH_2Cl_2$ is monomeric and represents the first experimentally well determined molecular structure of a monomeric trifluoro-chalcogenite anion. Similarly, $[((C_6H_5)_3P)_2N][SeF_5]$ represents the first example of a structure containing a well isolated undistorted SeF_5^- anion. The NMR and the vibrational spectra and their assignments were re-examined and corrected by comparison with high level theoretical calculations. Whereas the previously published normal coordinate analysis of SeF_5^- is correct, that for $SeOF_3^-$ needs major revision. The first crystal structures of a well isolated undistorted

SeF_5^- and of an oxotrifluorochalcogenite anion are reported. The pair-wise substitution of two fluorine atoms by a doubly bonded oxygen atom reduces the CN of Se from 6 to 4, and the presence of a sterically active free valence electron pair on Se has a strong influence on the bonding of the fluorine ligands. We have developed a composite approach to the prediction of the thermodynamic properties of molecules is based on CCSD(T) calculations extrapolated to the complete basis set limit plus the inclusion of additional corrections. This approach was used to calculate the heats of formation of SeF_5^-, SeO_2F^-, and $SeOF_3^-$ as well as those of SeF_4, SeO_2, and $SeOF_2$.

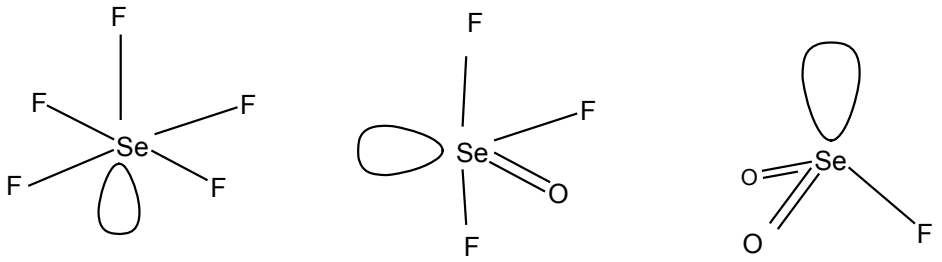

Structures and Heats of Formation of Simple Alkaline Earth Metal Compounds: Fluorides, Chlorides, Oxides, and Hydroxides for Be, Mg, and Ca Compounds containing the alkaline earth metals are commonly occurring substances in nature (calcium and magnesium are the fifth and eighth most abundant elements in the Earth's crust) and are used on a daily basis as part of the chemical industry. We are particularly interested in the thermochemical properties of the chlorides, fluorides, oxides and hydroxides of Be, Mg and Ca. Magnesium hydroxide is the main component of milk of magnesia. Magnesium oxide is used for lining furnaces, and calcium hydroxide (slaked lime) is the principal ingredient in plaster and mortar. Calcium chloride absorbs water from the air and it is used in the prevention of dust on roads, coal, and tennis courts and also as a drying agent in the laboratory. The alkaline earth monoxides play an important role in flame chemistry, in fuels (MgO) and possibly in stellar atmospheres. These are just a few examples of the importance of the alkaline earth compounds under study. The gas phase alkaline earth compounds are highly reactive species and the composition of the vapors is very complex, especially for the oxides and hydroxides. Geometry parameters, frequencies, heats of formation, and bond dissociation energies are predicted for the simple alkaline earth (Be, Mg and Ca) fluorides, chlorides, oxides and hydroxides at the coupled cluster theory [CCSD(T)] level including core-valence correlation with the aug-cc-pwCV*n*Z basis sets up to $n = 5$ in some cases. Additional corrections (scalar relativistic effects, vibrational zero-point energies, and atomic spin-orbit effects) were necessary to accurately calculate the total atomization energies and heats of formation. The calculated geometry parameters, frequencies, heats of formation, and bond dissociation energies are compared with the available experimental data and are in good agreement with reliable experimental results. For a number of these alkaline earth compounds, the experimental geometries and energies are not reliable. MgF_2 and BeF_2 are predicted to be linear and CaF_2 is predicted to be bent. BeOH is predicted to be bent, whereas MgOH and CaOH are linear. The OBeO angle in $Be(OH)_2$ is not linear and the molecule has C_2 symmetry. The heat of formation at 298 K for MgO is calculated to be 32.3 kcal/mol and the bond dissociation energy at 0 K is predicted to be 61.5 kcal/mol. The set of calculated values provides a consistent set of thermodynamic data for these commonly used alkaline earth compounds.

Why $[P(C_6H_5)_4]^+N_3^-$ and $[As(C_6H_5)_4]^+N_3^-$ are Ionic Salts and $Sb(C_6H_5)_4N_3$ and $Bi(C_6H_5)_4N_3$ are Covalent Solids Numerous examples are known where molecules are covalent in the gas

phase, while in the solid state they have ionic structures. Typical examples are PCl_5, N_2O_5, Cl_2O_6 or FNO. The energy difference, ΔE, between the ionic solid and the covalent gas can be determined by a simple Born-Fajans-Haber cycle. This energy difference is given by the sum of the bond dissociation energy of the covalent gas when it separates into two free radical fragments, the electron affinity of the more electronegative fragment, the first ionization potential of the more electropositive fragment, and the lattice enthalpy term, $-\Delta H_L$, obtained by appropriate correction of the lattice energy, $-U_L$, released when the resulting anion and cation form the ionic solid. The cases where closely related molecules can exhibit in their solid state either ionic or covalent structures are much less common and are not as well understood. It is commonly assumed that the governing factors in such cases are the maximum coordination numbers of the central atoms and the lattice and sublimation energies. To test the validity of these assumptions in a quantitative manner, we selected the $M(C_6H_5)_4N_3$ series, where M = P, As, Sb, and Bi. A recent crystallographic study has shown that, in the solid state, $P(C_6H_5)_4N_3$ and $As(C_6H_5)_4N_3$ have ionic $[M(C_6H_5)_4]^+N_3^-$ type structures, whereas $Sb(C_6H_5)_4N_3$ exists as a pentacoordinated covalent solid. Using the results from density functional theory, lattice energy (VBT) calculations, sublimation energy estimates, and Born-Fajans-Haber cycles, it is shown that the maximum coordination numbers of the central atom M, the lattice energies of the ionic solids, and the sublimation energies of the covalent solids have no or little influence on the nature of the solids. Unexpectedly, the main factor determining whether the covalent or the ionic structures are energetically favored, is the first ionization potential of $[M(C_6H_5)_4]$. The calculations show that at ambient temperature the ionic structure is favored for $P(C_6H_5)_4N_3$ and covalent structures are favored for $Sb(C_6H_5)_4N_3$ and $Bi(C_6H_5)_4N_3$, while $As(C_6H_5)_4N_3$ presents a borderline case.

Tetrakis(dimethylamido) **Hafnium Adsorption and Reaction on Hydrogen-Terminated Si(100) Surfaces** Hafnium oxide (HfO_2) is being used as a gate oxide in lieu of a SiO_2 insulating layer in the 45 nm technology node for metal oxide semiconductor field effect transistors (MOSFET), reducing leakage current, heat dissipation and power consumption, as well as increasing device reliability. Among all the high κ candidates, HfO_2 is generally accepted as the best material for this application due to its relatively high κ value (κ = 20-25), high band gap (E_g: ~5.6 eV), and thermodynamic stability on Si. The interfacial structure and chemistry are of special interest because the channel is formed very near this layer and is affected by impurities, dangling bonds, and trapped charges at the interface. There are a number of approaches to the formation of thin films of metal oxides for semiconductor applications. Atomic layer deposition (ALD) has an advantage over chemical vapor deposition (CVD) in that it can produce smooth films with more uniform chemical compositions over large areas. It involves exposure of the substrate to alternate cycles of a gaseous organometallic precursor and an oxidizing or reducing reactant. In principle, each step is self-limiting in that adsorption of the precursor stops after the available surface reactive sites are consumed so that one is able to effectively control the thickness at the atomic scale. Low temperature ALD is of special interest for semiconductor backend processing, thin film deposition on temperature sensitive substrates such as fabrics, plastic semiconductor substrates used in non-volatile memory organic field effect transistors and single-wall carbon nanotube field effect transistors, where the process temperatures are required to be below 150 ºC.

The most popular Hf precursors for ALD at present are hafnium alkylamides, due to the relatively weak Hf−N bond and their high volatility, which enables efficient deposition at relatively low temperatures. Hafnium alkylamides can be used as the gaseous precursor for both the gate and the oxide. The adsorption and reaction of *tetrakis(dimethylamido)hafnium* (TDMAH) on hydrogen terminated Si(100) were studied by using *in situ* attenuated total reflectance Fourier transform infrared spectroscopy (ATR-FTIR), transmission IR and quadrupole mass spectrometry (Q-MS). Surface and gas phase reactions were investigated at temperatures between 25 ºC and 300 ºC. Density functional theory (DFT) calculations benchmarked by coupled cluster theory (CCSD(T)) calculations on small models were performed for gas phase decomposition via intramolecular insertion and β-hydride elimination as well as the adsorption and reaction of TDMAH onto a hydrogen terminated Si(100) surface. N-Si and CH_2-Si bonds due to reactions on the Si windows were observed in transmission IR, while N-Ge and CH_2-Ge bonds on a Ge internal reflectance element (IRE) were observed by ATR-FTIR at 25 ºC and 100 ºC. Also observed were the formation of Hf-H bonds and three-member ring species on the Si surface; the former was confirmed by a control D_2O exchange reaction experiment. Both transmission IR and Q-MS indicated the presence of decomposition products dimethylamine (DMA) and N-methyl methyleneimine (MMI). The calculated bond dissociation energies (BDE) at the CCSD(T)/CBS level roughly follow the order of Hf-O > Hf-N > N-H, C-H, Si-N > Si-H, Si-C > N-C, Hf-H > Hf-Si, and the BDEs of the same chemical bond can vary substantially in different molecules. The interface is predicted by DFT calculations to involve Hf-Si, Hf-N-Si and/or HfNC-Si bonds. TDMAH decomposition products, such as MMI can form a C-Si or N-Si bond with the silicon surface. The combined experimental and theoretical results suggest that insertion and β-hydride elimination reactions can occur during bidenate chemisorption on the H-Si(100) surface by forming N-Si bonds. This work provides a detailed mechanism for the ALD process using TDMAH.

Tetrakis(ethylmethylamido) **Hafnium Adsorption and Reaction on Hydrogen-Terminated Si(100) Surfaces** The surface chemistry of the hafnium based ALD precursor, *tetrakis(ethylmethylamido) hafnium* (TEMAH), on hydrogen terminated Si (100) was studied for comparison with the previously reported *tetrakis(dimethylamido) hafnium* (TDMAH) results by *in situ* attenuated total reflectance Fourier transform infrared spectroscopy (ATR-FTIR) and *in vacuo* x-ray photoelectron spectroscopy (XPS). The adsorption and reaction experiments were investigated at substrate temperatures between 25 ºC and 400 ºC. Gas phase products were detected by *in situ* transmission FTIR. Density functional theory (DFT) calculations were performed for gas phase decomposition as well as the adsorption and reaction of TEMAH onto a hydrogen terminated model of a Si(100) surface. Our studies show that reactions during the initial steps of HfO_2 ALD using TEMAH and H_2O/D_2O involve complex processes. The formation of cyclo species containing alkyl C on Hf formed by a intramolecular insertion reaction and Hf-H species formed by β hydride elimination on the surface were identified by XPS at temperatures > 270 °C and a partial pressure of about 0.02 Torr for the former and ATR-FTIR at 100 °C and 0.1 Torr, for the latter. The latter was confirmed by a TEMAH/D_2O reaction experiment, supporting the previous observations of Hf-H species for TDMAH. The observation of an alkyl C on Hf as a proposed cyclo species, is sensitive to experimental conditions such as residence time, pressure, and temperature. Decompositions at higher pressures had an increased reaction rate. Transmission FTIR detected the formation of the gas phase products ethylmethylamine (EMA) and methylethyleneimine (MEI) or ethylmethyleneimine (EMI). DFT

calculations predicted the interface between the adsorbed molecules and H-Si(100) to involve Hf-Si, Hf-N-Si and/or Hf-N-C-Si bonds. The formation of bridged Si-N interfacial bonds provides a thermodynamically allowable way to generate these surface species and is supported by the observation of a N 1s XPS peak associated with Si-N. Interfacial formation of a N-Si bond is exothermic, -21.2 ± 1.3 kcal/mol from analysis of the growth of the thin film and -20 to -18 kcal/mol by our DFT calculations. The insertion reaction forming alkyl C on Hf has a reaction barrier of about 40 ± 3 kcal/mol from our chemical vapor deposition film growth experiments, entirely consistent with values of 36 to 40 kcal/mol from our DFT calculations. The results suggest that substantial care must be taken in the preparation of the surface, the substrate temperature, and the reagent pressure in the ALD of TEMAH if one wants to generate defect-free silicon surfaces with Hf interfaces. The deposition of the Hf will have to be carefully controlled to avoid the introduction of significant carbon impurities into the interface. A number of our experiments were carried out under conditions similar to those used in an actual ALD manufacturing process and the results show that this can lead to additional complexity in the products that are formed.

HfO_2 Films from the CVD of Hafnium (IV) tert butoxide. We also studied the undulating topography of HfO_2 thin films deposited in a meso-scale reactor using hafnium (IV) tert butoxide as the precursor. Chemical vapor deposition (CVD) is an important technique in thin film deposition and is widely applied in thin film layers or coatings for microelectronic devices, micro-electro-mechanical systems (MEMS), hard drive read/write heads, anti-corrosion layers, and other related technologies. HfO_2 was deposited by chemical vapor deposition on Si, native SiO_2, and borosilicate glass surfaces using hafnium (IV) tert butoxide in a meso-scale flow reactor. Undulating thin film topographies were observed by atomic force microscopy on all substrates with peak-to-peak periods between 10 to 25 nm in the presence of a temperature gradient perpendicular to flow of 25 ºC/mm. A computational fluid dynamic model suggests the phenomenon originates from buoyancy driven roll type flow. The thickness uniformity and roughness of the films depended on the flow rate, reactor temperature, and the substrate type. The depletion problem common in horizontal reactors was found to be tunable with different precursor supply flow rates. The periodicity of the rolls cannot be controlled very well by flux or other experimental parameters at this time and further study of this phenomenon is needed.

Bonding and microstructural stability in $Ni_{55}Ti_{45}$ studied by experimental and theoretical methods The NiTi family of shape memory alloys is an important structural material as it undergoes a thermally induced martensitic phase transformation between the high temperature, high symmetry rigid austenitic cubic phase (*B2*, $Pm\bar{3}m$) and the low temperature, low symmetry ductile martensitic monoclinic phase (*B19'*, $P2_1/m$). Upon cooling below the martensitic transformation temperature, unstrained shape-memory alloys have a twinned microstructure. When placed under stress, the twins reorient along the direction of applied stress, permitting easy deformation. When heated above the austenite transition temperature, the austenite phase is maintained and the alloy reverts to the original shape. Shape memory alloy activated structures have been extensively studied by the aerospace industry and have been used for such applications as generalized flow control, adaptive inlets and nozzles, variable geometry chevrons, variable chamber fan blades, and flaps and other hinged components. These examples capitalize upon the large reversible strain change inherent in typical near equi-atomic NiTi alloys. Although there has been extensive research on the shape memory properties of near equi-

atomic NiTi alloys, little attention has been paid to other interesting regions of the phase diagram.

Spiral orbit tribometry (SOT) experiments performed on the $Ni_{55}Ti_{45}$ Abbott Ball® bearing coated with 28.6 μg of Penzane2001-A® showed good bearing service lifetimes in rolling contact for this alloy, indicating it to be a candidate material for ball-bearing applications where traditional bearing materials such as tool steels cannot be used. SEM and TEM imaging was used to characterize the phases within the microstructure of the alloy. From these images, finely dispersed Ni_4Ti_3 precipitates, $Ni_2Ti_4O_x$ oxide phases, and low-angle NiTi grain boundaries were identified. A secondary Ni_3Ti phase was also identified, with a sub-structure containing stacking faults and dislocations. The presence of secondary phase particles and precipitates in the microstructure play a role in the dimensional stability in this unique alloy. DFT calculations show the d orbital character of the band structure and charge density of Ni_3Ti to be highly symmetric as compared to the less symmetric d orbital character of the NiTi band structure. The DOS from UPS experiments matches closely with the predicted DOS from DFT calculations. Overlaying the calculated DOS for each of the phases with the experimentally measured DOS shows that the experimental curve is not due to any pure phase, but rather to a superposition of different phases, indicating that the near-surface region of the bearing contains Ni-rich precipitates. Our DFT energy calculations are consistent with the formation of Ni rich particles in terms of the energies of the bulk phases. The calculated energies of formation for Ni_4Ti_3 and Ni_3Ti as well as reactions with excess Ni present show that these phases are more stable than the pure metals or NiTi. Charge density plots revealed negative charge accumulation around Ni sites in NiTi and Ni_4Ti_3, with Ni_3Ti displaying no preference for charge transfer due to the double hexagonal stacking pattern.

Although Ti bulk-phase alloys have not exhibited positive lubrication response under previous tribological testing with organic fluids, Ni bulk-phase alloys do exhibit positive lubrication response under similar conditions. This leads to the conclusion that there must be a Ni concentration above which the NiTi alloy should become favorable for lubrication conditions. We hypothesize that the mixed phase composition of the bearing surface and the Ni-rich composition of the alloy are both factors in the positive lubrication behavior of $Ni_{55}Ti_{45}$. The energy calculations clearly show that Ni rich phases for alloys derived from Ni and Ti can be formed in the presence of excess Ni which can be generated by oxidation of the Ti in the original NITi alloy. The delocalized metallic bonding found in the density of states calculations and the negative charge accumulation at Ni lattice sites shown in the charge density plots could be responsible for the improved lubrication behavior. Further investigation of the interactions of lubricant molecules with Ni_4Ti_3, Ni_3Ti, and NiTi phases will provide additional insight to the nature of the tribological performance in this system. A quantitative understanding of the tribochemistry at the molecular level of this or any alloy requires further study with the inclusion of a wide range of phenomena, which we are currently beginning to address.

Broader Impacts

Both the Dixon and Gole groups have significant numbers of undergraduate researchers. The Gole group has 6 undergraduates, 2 of whom are women. The Dixon group had 9 undergraduate students (1 woman) in the Fall 2010 and Spring 2011 semesters. The Dixon group sponsored 6

REU students (2 women) from non REU funding during the summer of 2010. There are 8 graduate students (3 women, 1 minority) in the research group. There are two postdoctoral fellows (1 woman) in the group. Two undergraduates (1 woman) won two of the 3 upper level UA Chemistry Department Awards. Two students (1 woman) were named Goldwater Scholars. Five of the 15 Randall Undergraduate Research Awards were awarded to students working in the Dixon group including 3 women and one student was awarded the Pettus Randall Scholarship for outstanding research by a student in the Computer Based Honors Program at UA. Dixon was named the 2011 Burnum Award winner at The University of Alabama. The Award is presented annually to a professor who is judged by a faculty selection committee to have demonstrated superior scholarly or artistic achievements and profound dedication to the art of teaching. The results from the research are being used in a Freshman Learning Community at UA taught by Dixon on Energy and the Environment.

The chief goal of this program is the acquisition of new knowledge on nanostructures for controlling chemical reactivity,such that this knowledge can be applied directly to the generation of new technologies that will benefit the national economy, the security of the nation, and the environment. These include splitting water for the production of hydrogen for the transportation sector. The development of economically viable methods for energy production with direct solar energy and minimal environmental impact to replace the combustion of carbon-based fuels is one of the scientific grand challenges of the 21st Century and this proposal will aid in the development of new technology platforms based on nanoparticles to address these issues. This work will have a strong impact on the design of new photocatalytic processes involving TiO_2, which can be used in removing organic contaminants or improving reaction selectivity. In addition, the studies carried out in this project are leading to an improved understanding of how TiO_2 nanoparticles can be used to split H_2O using solar energy to produce H_2 which might be used to power a fuel cell. Extensive thermodynamic data were generated for use in a broad range of higher scale modeling efforts including the industrial synthesis of TiO_2 particles, atmospheric chemistry in the troposphere and stratosphere, and combustion chemistry. The sensitive and selective sensors developed as part of this project will benefit the national economy, improve energy and national security, and be useful in environmental applications. In addition, such sensors have potential applications in the areas of health, biomedical, and law enforcement. The IHSAB (inverse hard/soft acid/base) model promises to have a significant impact on sensor design as it links chemical selectivity and the mechanism of sensor response for doped semiconductor sensors. The IHSAB model provides a simple-to-use prescription for sensor design which relates the physics and chemistry of specific nanostructure interfaces in microporous extrinsic semiconductor channels to sensor activity. The model combines the basic tenants of acid/base chemistry and semiconductor physics to form a road map for the implementation of readily constructed, cost effective, rapidly responding deployable devices sensitive to the ppb level.

Publications

Gole, J. L.; Ozdemir, S. “Nanostructure Directed Physisorption vs.Chemisorption at Semiconductor Interfaces: the Inverse of the Hard-Soft Acid-Base (HSAB) Concept,” *ChemPhysChem*, **2010**, *11*, 2573–2581.

Wang, T. –H.; Navarrete-López, A. M.; Li, S.; Dixon, D. A.; Gole, J. L. "Hydrolysis of $TiCl_4$: The Initial Steps in the Production of TiO_2," *J. Phys. Chem. A*, **2010**, 114, 7561–7570.

Wang, T.-H.; Fang, Z.; Gist, N. W.; Li, S.; Gole, J. L.; Dixon, D. A. "The Potential Energy Surfaces for the Hydrolysis of the Ground and First Excited States of TiO_2 Nanoclusters," *J. Phys. Chem. C*, **2011**, *115*, 9344-9360.

Wang, T.-H.; Dixon, D. A.; Henderson, M. A. "C-C and C-Heteroatom Bond Dissociation Energies in $CH_3R'C(OH)_2$: Energetics for Photocatalytic Processes of Organic Diolates on TiO_2 Surfaces," *J. Phys. Chem. C,* **2010**, 114, 14083–14092.

Wang, T.-H.; Gole, J. L.; White, M. G.; Watkins, C.; Street, S. C.; Dixon, D. A. "The Surprising Oxidation State of Fumed Silica and the Nature of Water Binding to Silicon Oxides and Hydroxides," *Chem. Phys. Lett.* **2011**, *501*, 159–165.

Ozdemir, S.; Gole, J. L. "A Phosphine Detection Matrix Using Nanostructure Modified Porous Silicon Gas Sensors," *Sensors and Actuators B*, **2010**, *151*, 274-280

Gole, J. L.; Ozdemir, S. "Efficient Nanostructure Modified Interfaces for Array-based Sensing Based on the Novel Application of Hard/Soft Acid/Base Interactions," *Phys. Stat. Solidi C*, **2011**, *8*, 1833-1836.

Gole, J. L; Ozdemir, S. "Novel Concept for the Formation of Sensitive, Selective, Rapidly Responding Conductometric Sensors," *MRS Proc*, **2010**, 1253-K07-05

Gole, J. L.; Ozdemir, S.; Prokes, S. M.; Dixon, D. A., "Active Nanostructures at Interfaces for Photocatalytic Reactors and Low-power Consumption Sensors," *MRS Proc.* **2010**, 1257-O09-04.

Wang, J.; Mao, B.; Gole, J. L.; Burda, C., "Visible-light-driven Reversible and Switchable Hydrophobic to Hydrophilic Surfaces: Correlation with Photocatalysis", *Nanoscale*, **2010**, *2*, 2257-2261.

Vasiliu, M.; Li, S.; Feller, D.; Gole, J. L.; Dixon, D. A. "Structures and Heats of Formation of Simple Alkaline Earth Metal Compounds: Fluorides, Chlorides, Oxides, and Hydroxides for Be, Mg, and Ca," *J. Phys. Chem. A*, **2010**, *114,* 9349–9358

Christe, K. O.; Dixon, D. A.; Grant, D. J.; Haiges, R.; Tham, F. S.; Vij, A.; Vij, V.; Wang, T.-H.; Wilson, W. W. "Dinitrogen Difluoride Chemistry. Improved Syntheses of *cis*– and *trans*–N_2F_2 , Synthesis and Characterization of $N_2F^+Sn_2F_9^-$, Ordered Crystal Structure of $N_2F^+Sb_2F_{11}^-$, High-Level Electronic Structure Calculations of *cis*-N_2F_2, *trans*-N_2F_2, $F_2N{=}N$, and N_2F^+, and Mechanism of the trans-cis Isomerization of N_2F_2," *Inorg. Chem*. **2010**, *49*, 6823-6833.

Grant, D. J.; Wang, T.-H.; Vasiliu, M.; Dixon, D. A.; Christe, K. O., "The F^+ and F^- Affinities of Simple N_xF_y and O_xF_y Compounds," *Inorg. Chem.* **2011**, *50*, 1914-1925.

Li, K.; Li, N.; Li, S.; Dixon, D. A.; Klein, T. M. "Tetrakis(dimethylamido) Hafnium Adsorption

and Reaction on Hydrogen-Terminated Si(100) Surfaces," *J. Phys. Chem. C*, **2010**, *114,* 14061–14075.

Gole, J. L; Ozdemir, S."Nanostructure Directed Gas-Surface Physisorption Based on Selective Modification of Nanopore Coated Micropores", *ECS Trans*., in press, 2011

Ozdemir, S.; Osburn, T.; Gole, J. L." A Nanostructure Modified porous Silicon Detection Matrix for NO with Demonstration of Transient Conversion of NO to NO_2," *J. Electrochem. Soc.* **2011**, *158*, J201-J207

Li, K.; Li, S.; Li, N.; Klein, T. M. Dixon, D. A.; "*Tetrakis(ethylmethylamido)* Hafnium Adsorption and Reaction on Hydrogen-Terminated Si(100) Surfaces," *J. Phys. Chem. C* WEB ASAP 8 2011 DOI: 10.1021/jp111600v

Li, K.; Zhang, L.; Dixon, D. A.; Klein, T. M., "Undulating Topography for HfO_2 Thin Films Deposited in a Meso-Scale Reactor using Hafnium (IV) tert butoxide," *AIChE Journal*, WEB Online Feb. 16, 2011 DOI: 10.1002/aic.12504

Christe, K. O.; Dixon, D. A.; Haiges, R.; Hopfinger, M.; Jackson, V. E.; Klapötke, T. M.; Krumm, B.; Scherr, M,. "Seleium(IV) Fluoride and Oxofluoride Anions," *J. Fluorine Chem*. **2010**, *131*, 791-799

Christe, K. O.; Haiges, R.; Boatz, J. A.; Jenkins, H. D. B.; Garner, E. B.; Dixon, D. A., "Why are $[P(C_6H_5)_4]^+N_3^-$ and $[As(C_6H_5)_4]^+N_3^-$ Ionic Salts and $Sb(C_6H_5)_4N_3$ and $Bi(C_6H_5)_4N_3$ are Covalent Solids? A Theoretical Study Provides an Unexpected Answer," *Inorg. Chem.* **2011**, *50*, 3752–3756

Stott, A. C.; Brauer, J. I.; Garg, A.; Pepper, S. V.; Abel, P. B.; DellaCorte, C.; Noebe, R. D.; Glennon, G.; Bylaska, E.; Dixon, D. A.,"Bonding and microstructural stability in $Ni_{55}Ti_{45}$ studied by experimental and theoretical methods," *J. Phys. Chem. C*, **2010**, *114,* 19704–19713

Presentations:

Ogden, A., Gole, J. L., Fedorov, A. G., "Hybrid Nanostructured TiO_2 Electrodes for Photocatalytic Hydrogen Production", 3rd Annual GCOE International Energy Conference, Ishigaki, Japan, Dec. 9-14, 2010.

Gole, J. L.; Ozdemir, S., " Novel Concept for the Formation of Sensitive, Selective, Rapidly Responding Conductometric Sensors", Microfabricated and Nanofabricated Systems for MEMS/NEMS 9, 218th Electrochemical Society Meeting, Oct. 10-15, 2010, Las Vegas, NV.

Gole, J. L.; Ozdemir, S., "Nanostructure Directed Gas-Surface Physisorption Based on Selective Modification of Nanopore Coated Micropores", Pits and Pores, New Materials and Applications 218th Electrochemical Society Meeting, Oct. 10-15,2010, Las Vegas, NV.

Gole, J. L., "Selectivity Improvements and Response Time Scale of Porous Silicon Conductometric Gas Sensors", 218th Electrochemical Society Meeting, Oct. 10-15,2010, Las Vegas, Neveda, in Chemical Sensors 9- Chemical and Biological Sensors and Analytical Systems

Gole, J. L., "Active Nanostructure Directed Processes at Interfaces": Speaker and Session Chair, Nanopackaging, " A General Model for Sensor and Microreactor Design on Semiconductor Interfaces", Nanoporous Materials, Nano Science and Technology- Dalian, China, October 23-26,2011, Keynote.

Gole, J. L., "Active Nanostructure Directed Processes at Interfaces"Villa Conference on Interactions Among Nanostructures, April 21-25, 2011,Las Vegas, Nevada, Invited Talk,

Dixon, D. A. "Computational Chemistry Undergraduate Research at UA," High School Advisory Board, The University of Aalabama, Sept. 13, 2010.

Dixon, D. A., "Computational Chemistry in a Distributed Computing Environment," University of Alabama-Birmingham, Cyberinfrastructure Day, 2010, Birmingham, AL, September, 15, 2010, Invited Lecture.

Dixon, D. A., Chen, M.; Stott, A.C.; Li, S. "Management of Computational Chemistry Electronic Structure Data in the U.S.", ZCAM Workshop on Databases in quantum chemistry: Validation of methods and software and repositories of reference computational results, Zaragoza Spain, Sept. 22-24, 2010, Invited Lecture

Dixon, D. A. "Reliable prediction of molecular properties of fluorinated inorganic compounds", Symposium on Fundamental and Applied Inorganic Fluorine Chemistry and Their Impacts on Energy Conservation and the Environment, PacifiChem 2010, Honolulu, HI, Dec. 15-20, 2010. Invited Lecture.

Christe, K. O.; Dixon, D. A.; Grant, D. J.; Tham, F. S.; Vij, A.; Vij, V.; Wang, T.-H.; Wilson, W. W. ""Dinitrogen Difluoride Chemistry. Improved Syntheses of *cis*– and *trans*–N_2F_2 , Synthesis and Characterization of $N_2F^+Sn_2F_9^-$, Ordered Crystal Structure of $N_2F^+Sb_2F_{11}^-$, High-Level Electronic Structure Calculations of *cis*-N_2F_2, *trans*-N_2F_2, $F_2N{=}N$, and N_2F^+, and Mechanism of the trans-cis Isomerization of N_2F_2 Symposium on Fundamental and Applied Inorganic Fluorine Chemistry and Their Impacts on Energy Conservation and the Environment, PacifiChem 2010, Honolulu, HI, Dec. 15-20, 2010. Invited Lecture.

Dixon, D. A.; Christe, K. O.; Vasiliu, M.; Craciun, R.; Li, S.; Grant, D. J.; Jackson, V. E., "Recent Results on the Lewis Acidity Scale: Quantitative Fluoride Affinities", 20th Winter Fluorine Conference, St. Petersburg Beach, FL, Jan. 9-14, 2011. Invited Lecture.

Haiges, R.; Christe, K. O.;, Boatz, J. A.; Dixon, D. A., "Metal Fluorides as Precursors for Environmental Friendly Energetic Materials: Replacements for Lead Diazide," 20th Winter Fluorine Conference, St. Petersburg Beach, FL, Jan. 9-14, 2011. Invited Lecture.

Christe, K. O.; Dixon, D. A.; Grant, D. J.; Wang, T.-H.; Vasiliu, M., "Formation mechanism of NF_4^+ salts," 20th Winter Fluorine Conference, St. Petersburg Beach, FL, Jan. 9-14, 2011. Invited Lecture

Vasiliu, M.; Arduengo, A. J. III; Dixon, D. A., "Bond Energies in Models of the Schrock and Grubbs Metathesis Catalysts", 20th Winter Fluorine Conference, St. Petersburg Beach, FL, Jan. 9-14, 2011. Poster

Jackson, V. E.; Dixon, D. A.; Christe, K. O., "Thermochemical Properties of Seleniumoxofluorides", 20th Winter Fluorine Conference, St. Petersburg Beach, FL, Jan. 9-14, 2011. Poster

Dixon, D. A.; "Computational Studies of Catalytic Processes on Metal Oxides", Gordon Research Conference: Chemical Reactions at Surfaces, Feb. 6-11, 2011, Ventura CA, Invited Lecture

Dixon, D. A., "Reliable predictions of the properties of transition metal complexes and fluorinated compounds," Computers in Chemistry Division: ACS Award for Computers in Chemical and Pharmaceutical Research Award: Symposium in Honor of Thom Dunning, 241st ACS National Meeting, Anaheim, CA, Mar. 27-31, 2011. Invited Lecture

Dixon, D. A., 2011 SETCA Annual Meeting, Mississippi State, Starksville MS May 13-14, 2011. Invited Lecture

Dixon, D. A., LANSCE Summer School, Los Alamos National Lab, Los Alamos, NM, July 12-22, 2011, Invited Lecture.

Stott, A. C.; Abel, P. B.; DellaCorte, C.; Pepper, S. V.; Dixon, D. A., "Computational Studies of the NiTi Alloy System: Bulk, Supercell, and Surface Calculations", Fall 2010 MRS Meeting, Boston MA.

Li, S.; Kelley, M. S.; Guenther, C. L.; Dixon D. A., "Hydrolysis of Group VIB Transition Metal Oxide Clusters and Their Catalytic Activity in Methanol Partial Oxidation by Molecular Oxygen," Joint SERM/SWRM 2010 Regional ACS meeting, New Orleans, LA, Nov. 30-Dec. 4, 2010.

Wang, T.-H.; Fang, Z.; Gist, N. W.; Li, S.; Dixon, D. A.," Computational Study of the Hydrolysis Reactions of the Ground and First Excited Triplet States of Small TiO_2 Nanoclusters", Joint SERM/SWRM 2010 Regional ACS meeting, New Orleans, LA, Nov. 30-Dec. 4, 2010, Poster

Awards

Andrew Ogden, Georgia Tech, graduate student, Mechanical Engineering, 1st Place Presentation Award, Hydrogen production technologies and research forum, 3rd Annual GCOE International Energy Conference, Ishigaki, Japan. Dec. 9-14, 2010.

Kyle Smith, Georgia Tech, senior, Physics, Joyce M. and Glenn Burdick Award for Scholastic Achievement and Leadership. Spring 2011.

D. A. Dixon, 2011 Burnum Award, The University of Alabama. The Award is presented annually to a professor who is judged by a faculty selection committee to have demonstrated superior scholarly or artistic achievements and profound dedication to the art of teaching.

D. A. Dixon June 2010, DOE Hydrogen Program R&D Award for Outstanding Contributions to Hydrogen Storage Technologies

New Findings: 2010-2011

- Developed an entirely new approach to the design of novel, highly sensitive sensors and catalysts based on the inverse hard/soft acid base model (IHSAB). When coupled with the intrinsic properties of semiconductors, this model provides a fundamental new way to design sensors based on their ability to adsorb/desorb species and the way that electron injection can change the resistance of the material.

- Continue to demonstrate visible-light-driven reversible and switchable hydrophobic to hydrophilic nitrogen doped titania surfaces correlating this behavior with photocatalysis.

- Developed an improved understanding of an impact of the spray cooling of the electrode support surface upon deposition of nanoparticles during the formation of the Hybrid NanoPatterned and Spray-Coated Electrode (HNPSCE) structure.

- Demonstrated enhanced photocatalytic operational stability and hydrogen generation yield with new HNPSCE electrode structure.

- Developed new understanding of the mechanical and electrical properties of the HNPSCE system on nanoscale, as related to electrode structural morphology and processing parameters.

- Nitrogen-doped TiO_2 nanoparticles have been synthesized using sol-gel methods and subsequently transformed into anatase nanocubes at room temperature by aging in acidic solutions of NaF. This two-step synthesis allows for independent control over the dopant concentration and material morphology. The approach is simple and could advance the preparation of visible light active TiO_2 photocatalysts.

- Predicted the F^+ and F^- Affinities of Simple N_xF_y and O_xF_y Compounds to explain their reactivity and the chemistry of N_2F^+ salts.

- Developed new thermodynamic parameters for seleniumoxofluorides.

- Developed new understanding of the atomic layer deposition of hafnium organometallics relevant to the generation of HfO_2 surfaces for electronics applications.

- Generated improved understanding of the properties of Nitinol alloys for aerospace applications.